

An Efficient Decomposition of the Carleman Linearized Burgers' Equation.

Reuben Demirdjian*

U.S. Naval Research Laboratory, Monterey, CA, 93943, United States

Thomas Hogancamp

*U.S. Naval Research Laboratory, Monterey, CA, 93943, United States and
American Society for Engineering Education, Washington, D.C.*

Daniel Gunlycke

U.S. Naval Research Laboratory, Washington, DC, 20375, United States

(Dated: March 13, 2026)

Herein, we present a polylogarithmic decomposition method to load the matrix from the linearized 1-dimensional Burgers' equation onto a quantum computer. First, we use the Carleman linearization method to map the nonlinear Burgers' equation into an infinite linear system of equations, which is subsequently truncated to order α . This new finite linear system is then embedded into a larger system of equations with the key property that its matrix can be decomposed into a linear combination of $\mathcal{O}(\log n_t + \alpha^2 \log n_x)$ terms for n_t time steps and n_x spatial grid points. While the terms in this linear combination are not unitary, each can be implemented using a simple block encoding procedure. A numerical simulation is performed by combining our approach with the variational quantum linear solver demonstrating that accurate solutions are possible. Finally, a resource estimate shows that the upper bound of the Clifford and T gate counts scale like $\mathcal{O}(\alpha(\log n_x)^2)$ and $\mathcal{O}((\log n_x)^2)$, respectively. This is therefore the first explicit polylogarithmic data loading method with respect to n_x and n_t for a Carleman linearized system.

I. INTRODUCTION

Partial differential equations (PDEs) are ubiquitous in nearly all scientific and engineering disciplines, however, their solutions are rarely analytically known. Instead, PDEs are typically solved numerically using high performance computers along with discretization methods to find approximate solutions [1–3]. In computational fluid dynamics (CFD) and numerical weather prediction (NWP), the computational resources available can limit model accuracy by constraining the grid size of spatial and temporal discretizations [4]. A spatially coarse CFD or NWP model may be unable to resolve important small-scale features of the fluid (e.g. turbulence and convection) and instead rely on parameterization or closure methods to approximate their effects, ultimately leading to error growth that can eventually corrupt the solution [5–7]. Therefore, an increase in computational resources enables finer spatial discretizations, which may allow for fewer or more accurate parameterizations and thereby a more accurate solution [8].

Quantum computing is an emerging field that can exponentially speedup specific applications [9–11] such as solving linear systems of equations [12–15]. Since CFD models rely on solving nonlinear PDEs, the Carleman linearization method has been proposed to transform the original set of nonlinear PDEs into an infinite set of linear ordinary differential equations (ODEs), which are subsequently truncated into a finite set of linear ODEs [16–18]. The advantage of this method is that a quantum linear

system algorithm (QLSA) may be applied to solve the set of linear ODEs and thereby obtain an approximate solution to the original nonlinear PDE. However, there are a number of challenges that must be solved if this is to be done efficiently, and it is currently an open question whether this, or any other method of solving nonlinear PDEs, are viable on quantum computers [19–38].

One such challenge is the data loading problem for linear systems of equations. This can be understood by considering the variational quantum linear solver (VQLS) [12] – a variational technique used to solve linear systems of equations of the form $L\vec{x} = \vec{b}$ where $L \in \mathbb{C}^{N \times N}$ and $\vec{x}, \vec{b} \in \mathbb{C}^N$. The VQLS method, among other QLSAs, relies on the linear combination of unitaries [39], whereby $L = \sum_{l=0}^{N_s-1} c_l A_l$ for complex coefficients c_l and unitary matrices $A_l \in \mathbb{C}^{N \times N}$. While any square matrix L is guaranteed to have a decomposition of this form, the VQLS algorithm is only efficient if $N_s \sim \mathcal{O}(\text{poly}(\log N))$. This restriction comes from the fact that the number of circuits in the VQLS cost function scales like $\mathcal{O}(N_s^2)$ [17]. This means that N_s must have a practical bound; otherwise, the quantum advantage is lost simply by executing the large number of circuits to load the linear system. Similarly, each A_l circuit depth must also be bounded by $\mathcal{O}(\text{poly}(\log N))$, otherwise quantum advantage is again lost when preparing the individual circuits. Henceforth, we refer to the problem of finding a decomposition such that both the number of circuits N_s and the A_l circuit depths (or a block encoding thereof) are both bounded by $\mathcal{O}(\text{poly}(\log N))$ as the *decomposition problem*. This may also be thought of as the data loading problem, which is not generally efficient and therefore requires bespoke methods for each application [40–46].

* Reuben.Demirdjian.civ@us.navy.mil

Another challenge is that the conditions under which the Carleman linearization approach is applicable is currently a topic of research. In Liu *et al.* [16], they define the parameter R as the ratio of nonlinearity to dissipation finding that the Carleman linearization error converges to zero exponentially with increasing truncation order for $R < 1$. Conversely, for $R \geq 1$ they find that the truncation order must grow exponentially with time to bound the error. The latter result problematic because the size of a Carleman linearized system scales exponentially with the truncation order. That being said, their analytical analysis provides only an upper bound and they even numerically show that accurate solutions are possible in the $R \geq 1$ regime using small truncation orders. Furthermore, their analysis is limited to a specific class of dissipative systems. Jennings *et al.* [47] extended their analysis to a broader class of stable systems by defining independent R -numbers for each type of system. Their analysis allows for improved error bounds thereby extending the types of nonlinear dynamical systems that can be efficiently simulated with quantum computers. However, as was found in the Liu *et al.* [16] analysis, it may be that the bounds imposed by analytical analyses are too conservative, in which case learning what problems can be solved may come experimentally.

A. Contributions

In this study, we solve the decomposition problem for the 1-dimensional (1D) Carleman linearized Burgers' equation with periodic boundary conditions – a paradigmatic nonlinear PDE. Figure 1 illustrates the methods introduced here and contrasts them with the ones used in [16, 17]. Both the previous and proposed methods follow the same two initial steps, first the 1D Burgers' equation is discretized (box a) and then the Carleman linearization method is applied (box b). At this point, our approaches deviate. In the previous method, one would decompose the matrix A (box c) and then use a QLSA (like the VQLS) to obtain a solution (box d). However, there are no known poly($\log N$) decompositions for the basic Carleman linearized Burgers' equation [36] and therefore quantum advantage is lost. In contrast, the proposed method embeds the Carleman linearized 1D Burgers' equation into an even larger system of equations with matrix $A^{(e)}$ (box e). The benefit of this additional layer of complexity is that $A^{(e)}$ can be efficiently decomposed into poly($\log N$) terms (box f) that can be implemented into a QLSA using circuits with poly($\log N$) depths (box g). The proposed method therefore offers a quantum advantage when used in combination a QLSA that requires a linear combination of unitaries like VQLS (box d).

The key insights presented in this paper are two-fold: (1) the zero padding method that enables us to decompose the matrix into a polylogarithmic number of terms, and (2) an extension of the block encoding method, introduced in Gnanasekaran and Surana (2024) [48], that en-

ables us to efficiently block encode each term. Together, these two insights provide a polylogarithmic decomposition for the 1D Carleman linearized Burgers' equation. It is important to note that while the decomposition presented here is problem specific, we believe that the insights introduced can be generalized and applied to more complex problems.

This work is structured as follows: In Section II we present an overview of the relevant results from [48]. The Carleman linearized 1D Burgers' equation from [16] is derived in Section III and our zero padding approach is introduced in Section IV. Next, in Section V we derive an efficient decomposition for the zero padded matrix by splitting it into terms that are easily block encoded, which are subsequently presented in Section VI. Next, a resource estimation for our decomposition approach is performed in Section VII and shown to be efficient (polylogarithmic). Our approach is then combined with the VQLS method to perform a numerical simulation in Section VIII demonstrating that it can be used to find accurate solutions. Finally, we present our conclusions in Section IX and discuss implications.

II. OVERVIEW OF [48]

Define the tau basis $\mathbb{T} = \{\tau_0, \tau_1, \tau_2, \tau_3\}$ and the sigma (Pauli) basis $\mathbb{S} = \{\sigma_0, \sigma_1, \sigma_2, \sigma_3\}$ where

$$\tau_0 = |0\rangle\langle 0|, \tau_1 = |0\rangle\langle 1|, \tau_2 = |1\rangle\langle 0|, \tau_3 = |1\rangle\langle 1|,$$

and $\sigma_0 = \sigma_x, \sigma_1 = \sigma_y, \sigma_2 = \sigma_z$, and $\sigma_3 = I$.

Suppose we have a matrix $A \in \mathbb{C}^{N \times N}$, $N = 2^Q$ for some integer Q . In the tau basis there exists a unique decomposition $A = \sum_{l=0}^{N_\tau-1} c_l C_l$ for N_τ terms where $C_l = \bigotimes_{k=0}^{Q-1} \tau_{v_k}$, for $\tau_{v_k} \in \mathbb{T}$, $v_k \in \{0, \dots, 3\}$ and $c_l \in \mathbb{C}$. Similarly, in the sigma basis there exists a unique decomposition $A = \sum_{l=0}^{N_\sigma-1} d_l D_l$ for N_σ terms where $D_l = \bigotimes_{k=0}^{Q-1} \sigma_{w_k}$, for $\sigma_{w_k} \in \mathbb{S}$, $w_k \in \{0, \dots, 3\}$ and $d_l \in \mathbb{C}$. It is important to note that, while these decompositions always exist, the number of terms (N_τ and N_σ) may be exponential for an arbitrary matrix.

To circumvent this problem, [48–50] introduced a mixed tau and sigma set given by $\mathbb{P} = \{\rho_0, \rho_1, \rho_2, \rho_3, \rho_4\}$ where $\rho_0 = \tau_0, \rho_1 = \tau_1, \rho_2 = \tau_2, \rho_3 = \tau_3, \rho_4 = \sigma_3$. Using this new set, there exist non-unique decompositions of the form $A = \sum_{l=0}^{N_s-1} a_l A_l$ where $A_l = \bigotimes_{k=0}^{Q-1} \rho_{r_k}$, for $\rho_{r_k} \in \mathbb{P}$, $r_k \in \{0, \dots, 4\}$ and $a_l \in \mathbb{C}$. For specific matrices, [48] shows that there exist decompositions with $N_s = \mathcal{O}(\text{poly}(\log N))$, providing an exponential improvement compared to that of the tau or sigma basis alone. One challenge presented with this method, however, is that the A_l matrices are not unitary. To resolve this, [48] shows that each A_l can be systematically block encoded. Furthermore, they develop a method to implement these block encodings directly into VQLS. The following constructions are adapted from Section 4 of [48].

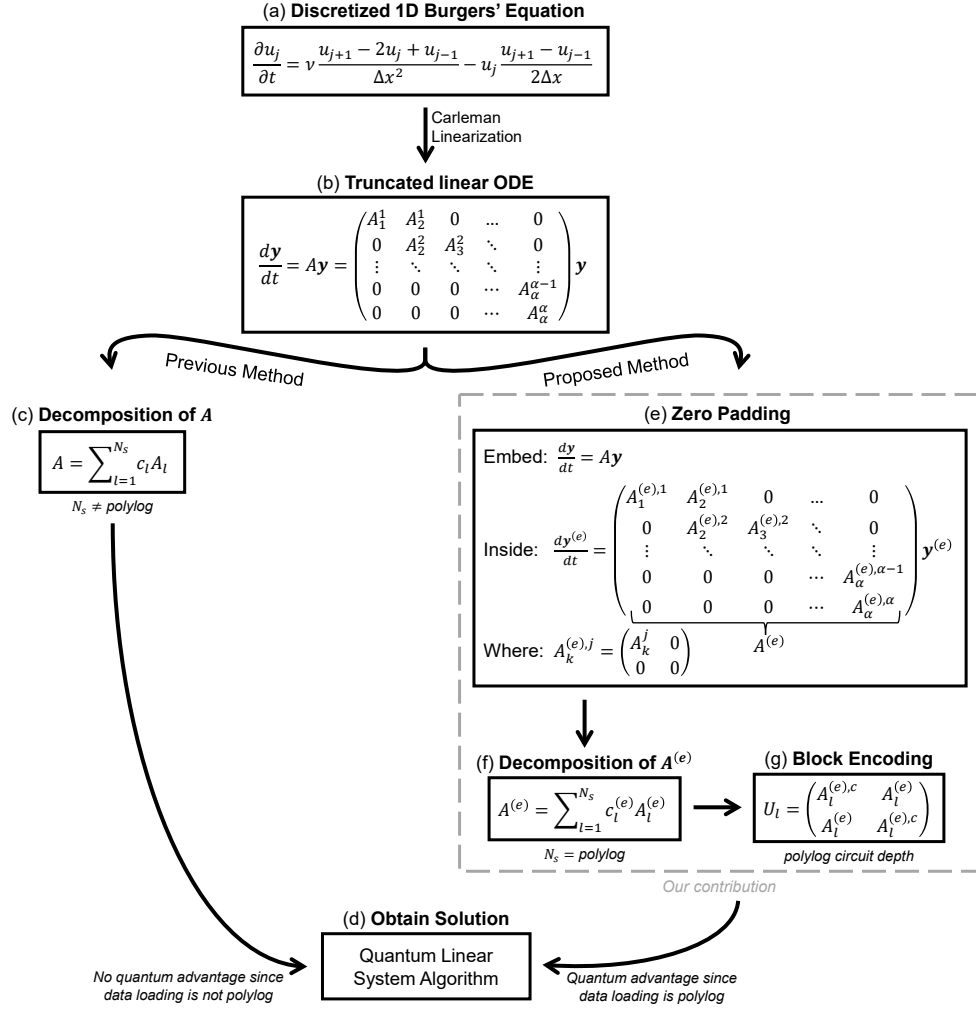


FIG. 1: An illustration comparing the method proposed in this study (boxes a,b,e,f,g,d) with the previous method (boxes a,b,c,d). (a) The spatially discretized 1D Burgers' equation. (b) The truncated Carleman linearized 1D Burgers' equation. (c) Decomposition of the Carleman linearized matrix A of which no known polylog decomposition exists [36]. Note that the time discretization step is skipped in this simplification. (d) A QLSA to solve the linear system. (e) The zero padding method whereby the original system of equations A are embedded in a larger system $A^{(e)}$. (f) The matrix $A^{(e)}$ is decomposed efficiently into $\text{poly}(\log N)$ terms. (g) Each $A_l^{(e)}$ matrix is block encoded with $\text{poly}(\log N)$ circuit depth.

Definition 1. Suppose $W \subset V$ where V is a Hilbert space. For a linear operator $F : W \rightarrow V$ that preserves inner products, the unitary operator $\overline{F} : V \rightarrow V$ is called a unitary completion when \overline{F} spans the whole space V and $\overline{F}|w\rangle = F|w\rangle \forall |w\rangle \in W$. Additionally, $F^c := \overline{F} - F$ is the unitary complement of F and is unique for a specific choice of \overline{F} given F .

Note that, while [48] uses the term unitary complement, we opted for the more general and widely used term unitary completion. Also, the unitary completion always exists and is not necessarily unique (see Def. 2 of [48] and Ex. 2.67 of [51]). Following Definition 1, Theorem 2 of [48] describes how to construct \overline{A}_l for decompositions in \mathbb{P} . If $A_l = \bigotimes_k \rho_{r_k}$, then $\overline{A}_l = \bigotimes_k \overline{\rho}_{r_k}$

where

$$\overline{\rho}_{r_k} = \begin{cases} \sigma_0, & \rho_{r_k} \in \{\rho_1, \rho_2\} \\ \sigma_3, & \rho_{r_k} \in \{\rho_0, \rho_3, \rho_4\} \end{cases}. \quad (1)$$

Therefore, each A_l may be block encoded with an associated unitary matrix $U_l \in \mathbb{C}^{2N \times 2N}$ by

$$U_l = \begin{pmatrix} A_l^c & A_l \\ A_l & A_l^c \end{pmatrix},$$

where we have followed the convention of [48] by encoding A_l in the upper right block instead of the upper left. Furthermore, Theorem 3 of [48] shows that U_l can be implemented using at most $Q = \log N$ single qubit gates

and a single $C^q X$ gate where $q \leq Q$. Finally, they derive efficient quantum circuits to calculate the local VQLS cost function based on this block encoding strategy.

III. CARLEMAN LINEARIZATION

The 1D Burgers' equation with periodic boundary conditions and domain length L_x is given by

$$\frac{\partial u}{\partial t} = \nu \frac{\partial^2 u}{\partial x^2} - u \frac{\partial u}{\partial x},$$

$$u(x, 0) = u^0(x), \quad u(0, t) = u(L_x, t),$$

where $u(x, t)$ is the fluid velocity, ν is the diffusion coefficient. This can be discretized into

$$\frac{\partial u_j}{\partial t} = \frac{\nu}{\Delta x^2} (u_{j+1} - 2u_j + u_{j-1}) - \frac{u_j}{2\Delta x} (u_{j+1} - u_{j-1}), \quad (2)$$

$$u_j(0) = u_j^0, \quad u_0(t) = u_{n_x}(t),$$

where Δx is the grid spacing and $\vec{u} = (u_0, \dots, u_{n_x-1})^T$ is the fluid velocity at each grid point. This can be rewritten in the form

$$\frac{\partial \vec{u}}{\partial t} = F_1 \vec{u} + F_2 \vec{u}^{\otimes 2}, \quad \vec{u}(0) = \vec{u}^0,$$

where $F_1 \in \mathbb{C}^{n_x \times n_x}$ and $F_2 \in \mathbb{C}^{n_x \times n_x^2}$. Following [16], the Carleman linearized 1D Burgers' equation with truncation order $\alpha = 2^r$ for integer r takes the form

$$\frac{d\vec{y}}{dt} = A\vec{y}, \quad (3)$$

$$\vec{y}(0) = ((\vec{u}^0), (\vec{u}^0)^{\otimes 2}, \dots, (\vec{u}^0)^{\otimes \alpha})^T,$$

where

$$A := \begin{pmatrix} A_1^1 & A_2^1 & 0 & \dots & 0 \\ 0 & A_2^2 & A_3^2 & \dots & 0 \\ \vdots & \dots & \ddots & \ddots & A_{\alpha}^{\alpha-1} \\ 0 & 0 & \dots & 0 & A_{\alpha}^{\alpha} \end{pmatrix}, \quad (4)$$

and $\vec{y} = (\vec{u}, \vec{u}^{\otimes 2}, \dots, \vec{u}^{\otimes \alpha})^T \in \mathbb{C}^{\Delta}$, $\Delta = \sum_{j=1}^{\alpha} n_x^j$ and $A \in \mathbb{C}^{\Delta \times \Delta}$. Furthermore, $A_j^j \in \mathbb{C}^{n_x^j \times n_x^j}$ and $A_{j+1}^j \in \mathbb{C}^{n_x^j \times n_x^{j+1}}$ are defined as

$$A_j^j := \sum_{l=0}^{j-1} I_{n_x}^{\otimes l} \otimes F_1 \otimes I_{n_x}^{\otimes j-l-1}, \quad (5a)$$

$$A_{j+1}^j := \sum_{l=0}^{j-1} I_{n_x}^{\otimes l} \otimes F_2 \otimes I_{n_x}^{\otimes j-l-1}, \quad (5b)$$

where $I_n := I^{\otimes \log n}$. Using the backward Euler discretization with n_t time steps, (3) becomes

$$L\vec{Y} = \vec{B}, \quad (6)$$

which is expanded into

$$\begin{pmatrix} I & 0 & \dots & 0 \\ -I & M & \dots & 0 \\ \vdots & \ddots & \ddots & \vdots \\ 0 & \dots & -I & M \end{pmatrix} \begin{pmatrix} \vec{y}^0 \\ \vec{y}^1 \\ \vdots \\ \vec{y}^{n_t-1} \end{pmatrix} = \begin{pmatrix} \vec{y}^0 \\ \vec{0}_{\Delta} \\ \vdots \\ \vec{0}_{\Delta} \end{pmatrix},$$

where $M = I - \Delta t A$, $L \in \mathbb{C}^{n_t \Delta \times n_t \Delta}$, $\vec{Y}, \vec{B} \in \mathbb{C}^{n_t \Delta}$, $\vec{0}_{\Delta}$ is the zero vector of size Δ , and $\vec{y}^m = \vec{y}(m\Delta t)$.

IV. ZERO PADDING

Following the approach of [48, 49], one would attempt to write the matrix in (4) as a linear combination of elements from \mathbb{P} . The sparsity and highly patterned structure of A suggests that this can be done efficiently. However, the non-square A_{j+1}^j terms create a serious technical impediment. To overcome this challenge, we embed (6) into a larger system in which judicious zero padding creates a convenient square block structure. First, we define $A_j^{(e),j} \in \mathbb{C}^{n_x^{\alpha} \times n_x^{\alpha}}$ by embedding the associated lower dimensional A_j^j matrices given by

$$A_j^{(e),j} := \rho_0^{\otimes \log n_x^{\alpha-j}} \otimes A_j^j$$

$$= \begin{pmatrix} A_j^j & 0_{n_x^j \times (n_x^{\alpha} - n_x^j)} \\ 0_{(n_x^{\alpha} - n_x^j) \times n_x^j} & 0_{(n_x^{\alpha} - n_x^j) \times (n_x^{\alpha} - n_x^j)} \end{pmatrix}, \quad (7)$$

where $j \in \{1, \dots, \alpha\}$ and $n_x = 2^s$ for an integer s . Similarly, we define $A_{j+1}^{(e),j} \in \mathbb{C}^{n_x^{\alpha} \times n_x^{\alpha}}$ terms by embedding the A_{j+1}^j matrix given by

$$A_{j+1}^{(e),j} := \begin{pmatrix} A_{j+1}^j & 0_{n_x^j \times (n_x^{\alpha} - n_x^{j+1})} \\ 0_{(n_x^{\alpha} - n_x^j) \times n_x^{j+1}} & 0_{(n_x^{\alpha} - n_x^j) \times (n_x^{\alpha} - n_x^{j+1})} \end{pmatrix}$$

$$= \rho_0^{\otimes \log(n_x^{\alpha-j-1})}$$

$$\otimes \sum_{l=0}^{j-1} \left[\left(\rho_0^{\otimes \log n_x} \otimes K(n_x^l, n_x) \right) \right. \quad (8)$$

$$\cdot \left. \left(\begin{pmatrix} F_2 \\ 0_{(n_x^2 - n_x) \times n_x^2} \end{pmatrix} \otimes I_{n_x}^{\otimes l} \right) \cdot K(n_x^2, n_x^l) \right]$$

$$\otimes I_{n_x}^{\otimes j-l-1},$$

where $K^{(a,b)} \in \mathbb{C}^{(ab \times ab)}$ denotes the commutation matrix. See Appendix B for (8)'s full derivation.

We can now define an analogous version of the matrix

A in (4) given by

$$\begin{aligned}
A^{(e)} &:= \begin{pmatrix} A_1^{(e),1} & A_2^{(e),1} & 0 & \dots & 0 \\ 0 & A_2^{(e),2} & A_3^{(e),2} & \dots & 0 \\ \vdots & \dots & \ddots & \ddots & A_\alpha^{(e),\alpha-1} \\ 0 & 0 & \dots & 0 & A_\alpha^{(e),\alpha} \end{pmatrix} \\
&= \sum_{j=1}^{\alpha} (\rho_{f(b_\alpha(j-1), b_\alpha(j-1))} \otimes A_j^{(e),j}) \\
&\quad + \sum_{j=1}^{\alpha-1} (\rho_{f(b_\alpha(j-1), b_\alpha(j))} \otimes A_{j+1}^{(e),j}),
\end{aligned} \tag{9}$$

where $A^{(e)} \in \mathbb{C}^{\alpha n_x^\alpha \times \alpha n_x^\alpha}$. Following [40], the function $f : \{0, 1\}^K \times \{0, 1\}^K \rightarrow \{0, 1, 2, 3\}^K$ is defined as $f(i_K, j_K) = f_{K-1} \dots f_0$ where each quaternary bit is calculated by $f_k = 2i_k + j_k$ for $i_K := i_{K-1} \dots i_0$, $j_K := j_{K-1} \dots j_0$ and $k = 0, \dots, K-1$. The function $b_\beta(j)$ maps the base-ten number $j \in \{1, \dots, \alpha\}$ to a binary number with $\log \beta$ digits with $\beta = 2^Q$ for some integer Q . Together, these functions are used to map row and column decimal indices into the quaternary bitstring $f_{K-1} \dots f_0$, allowing for the convenient shorthand notation: $\rho_{f_{K-1}} \otimes \dots \otimes \rho_{f_0}$. For clarity, Appendix A shows several examples.

We may now define the embedded system of equations, analogous to (6), as

$$L^{(e)} \vec{Y}^{(e)} = \vec{B}^{(e)}, \tag{10}$$

where

$$L^{(e)} = \begin{pmatrix} I & 0 & \dots & 0 \\ -I & M^{(e)} & \dots & 0 \\ \vdots & \ddots & \ddots & \vdots \\ 0 & \dots & -I & M^{(e)} \end{pmatrix}, \tag{11}$$

and $L^{(e)} \in \mathbb{C}^{\alpha n_t n_x^\alpha \times \alpha n_t n_x^\alpha}$, $\vec{Y}^{(e)} = (\vec{y}^{(e),0}, \dots, \vec{y}^{(e),n_t-1})^T$, $\vec{B}^{(e)} = (\vec{y}^{(e),0}, \vec{0}_{\alpha(n_t-1)n_x^\alpha})^T$, $M^{(e)} = I - \Delta t A^{(e)}$, and $\vec{y}^{(e),m} = ((\vec{u}^m), \vec{z}_1, (\vec{u}^m)^{\otimes 2}, \vec{z}_2, \dots, (\vec{u}^m)^{\otimes \alpha})^T$ for the m^{th} time step and $\vec{z}_j \in \mathbb{C}^{n_x^\alpha - n_x^j}$. Note that the structure of the $A^{(e)}$ matrix will force the \vec{z}_j -vectors to be zero. The process used to obtain (10) from (6) is a specific zero padding approach to embed the original Carleman linearized system into a larger dimensional system of equations. In this case, the zero padded system has a polylogarithmic decomposition as will be shown.

V. DECOMPOSITION OF $L^{(e)}$

We now demonstrate how to decompose $L^{(e)}$ from (11) into a linear combination of terms of the form

$$L^{(e)} = \sum_{l=0}^{N_s-1} c_l L_l \tag{12}$$

where $c_l \in \mathbb{C}$ and the terms $L_l \in \mathbb{C}^{\alpha n_t n_x^\alpha \times \alpha n_t n_x^\alpha}$ are tensor products of certain well-known unitary matrices with elements in \mathbb{P} . First, separate the identity blocks by

$$L^{(e)} = L_1^{(e)} - \Delta t L_2^{(e)}, \tag{13}$$

where

$$L_1^{(e)} = \begin{pmatrix} I & 0 & \dots & 0 \\ -I & I & \dots & 0 \\ \vdots & \ddots & \ddots & \vdots \\ 0 & \dots & -I & I \end{pmatrix},$$

and

$$L_2^{(e)} = \begin{pmatrix} 0 & 0 & \dots & 0 \\ 0 & A^{(e)} & \dots & 0 \\ \vdots & \ddots & \ddots & \vdots \\ 0 & \dots & 0 & A^{(e)} \end{pmatrix}.$$

Following [48], $L_1^{(e)}$ can be split into just $\log n_t + 1$ terms provided by

$$\begin{aligned}
L_1^{(e)} &= \left(\rho_4^{\otimes \log n_t} - \rho_4^{\otimes (\log(n_t)-1)} \otimes \rho_2 \right. \\
&\quad \left. - \sum_{j=2}^{\log n_t} \rho_4^{\otimes (j-2)} \otimes \rho_2 \otimes \rho_1^{\otimes (\log(n_t)-j+1)} \right) \\
&\quad \otimes \rho_4^{\otimes \log(\alpha n_x^\alpha)},
\end{aligned} \tag{14}$$

where $n_t = 2^m$ for an integer m . Next, we split $L_2^{(e)}$ by

$$L_2^{(e)} = \rho_4^{\otimes \log n_t} \otimes A^{(e)} - \rho_0^{\otimes \log n_t} \otimes A^{(e)}. \tag{15}$$

By evaluating (9) into (15) we obtain

$$L_2^{(e)} = L_{2a}^{(e)} + L_{2b}^{(e)}, \tag{16}$$

where

$$\begin{aligned}
L_{2a}^{(e)} &= \left((\rho_4^{\otimes \log n_t} - \rho_0^{\otimes \log n_t}) \right. \\
&\quad \left. \otimes \sum_{j=1}^{\alpha} (\rho_{f(b_\alpha(j-1), b_\alpha(j-1))} \otimes A_j^{(e),j}) \right),
\end{aligned} \tag{17a}$$

$$L_{2b}^{(e)} = \left((\rho_4^{\otimes \log n_t} - \rho_0^{\otimes \log n_t}) \otimes \sum_{j=1}^{\alpha-1} (\rho_f^{(b_\alpha(j-1), b_\alpha(j))} \otimes A_{j+1}^{(e),j}) \right). \quad (17b)$$

$L_2^{(e)}$ has two types of terms: (1) the $L_{2a}^{(e)}$ terms associated with $A_j^{(e),j}$, and (2) the $L_{2b}^{(e)}$ terms associated with $A_{j+1}^{(e),j}$. We handle their decompositions separately in the next two subsections.

A. Decomposition of $L_{2a}^{(e)}$

First, by inserting (5a) into (7) it can be seen that the $A_j^{(e),j}$ decomposition depends upon F_1 . Conveniently, the F_1 term can be decomposed into $2 \log n_x + 3$ elements of \mathbb{P} for the case of periodic boundary conditions provided by

$$\begin{aligned} \frac{\Delta x^2}{\nu} F_1 &= -2\rho_4^{\otimes s} + \rho_4^{\otimes(s-1)} \otimes (\rho_1 + \rho_2) \\ &+ \rho_1^{\otimes s} + \rho_2^{\otimes s} + \sum_{i=2}^s \rho_4^{\otimes(i-2)} \\ &\otimes \left(\rho_2 \otimes \rho_1^{\otimes(s-i+1)} + \rho_1 \otimes \rho_2^{\otimes(s-i+1)} \right), \end{aligned} \quad (18)$$

where $n_x = 2^s$. By inserting (18), (5a), and (7), into (17a) we can see that $L_{2a}^{(e)}$ is decomposed into a linear combination of purely elements from \mathbb{P} . It is therefore straightforward to calculate the VQLS cost function using the methods in [48].

B. Decomposition of $L_{2b}^{(e)}$

Next, we look at the $L_{2b}^{(e)}$ terms. From (8) it is plain to see that $A_{j+1}^{(e),j}$ depends upon the matrix $\begin{pmatrix} F_2 \\ 0_{(n_x^2 - n_x) \times n_x^2} \end{pmatrix}$. To gain some insight into the structure of this matrix, we consider the case for $n_x = 4$ shown in Appendix C. In general, the nonzero elements exist only in the first n_x -rows, and each of these rows has exactly two nonzero elements. We can therefore split this matrix into two terms given by

$$\begin{pmatrix} F_2 \\ 0_{(n_x^2 - n_x) \times n_x^2} \end{pmatrix} = -(F^+ - F^-)/(2\Delta x), \quad (19)$$

where F^+ contains the $u_j u_{j+1}$ terms and F^- contains the $u_j u_{j-1}$ terms from (2). These matrices can be decomposed into products of a diagonal matrix and a permutation matrix by

$$F^+ = \mathcal{D}P^+, \quad F^- = \mathcal{D}P^-,$$

where $\mathcal{D}, P^+, P^- \in \mathbb{C}^{n_x^2 \times n_x^2}$. The \mathcal{D} -matrix is defined by

$$\begin{aligned} \mathcal{D} &:= \begin{pmatrix} \rho_4^{\otimes \log n_x} & 0_{n_x \times (n_x^2 - n_x)} \\ 0_{(n_x^2 - n_x) \times n_x} & 0_{(n_x^2 - n_x) \times (n_x^2 - n_x)} \end{pmatrix} \\ &= \rho_0^{\otimes \log n_x} \otimes \rho_4^{\otimes \log n_x}. \end{aligned} \quad (20)$$

The permutation matrices P^+ and P^- are not unique since they may be written as

$$P^+ = \begin{pmatrix} F_2^+ \\ (F_2^+)^c \end{pmatrix}, \quad P^- = \begin{pmatrix} F_2^- \\ (F_2^-)^c \end{pmatrix},$$

where $F_2^+, F_2^- \in \mathbb{C}^{n_x \times n_x}$ are the unique positive and negative element positions of F_2 respectively (see Appendix C), and $(F_2^+)^c, (F_2^-)^c \in \mathbb{C}^{(n_x^2 - n_x) \times n_x^2}$ are their unitary complements, which are not unique by Definition 1. As shown in Appendix D, there exists a choice for $(F_2^+)^c$ and $(F_2^-)^c$ such that $P^+ = P_2^+ P_1$ and $P^- = P_2^- P_1$ for known P_1, P_2^+ and P_2^- . Their associated quantum circuits are

$$P_1 = \prod_{q=0}^{s-1} CX(s-q-1, 2s-q-1), \quad (21a)$$

$$P_2^+ = X_0 CX(0, 1) \left(\prod_{q=0}^{s-3} C^{q+2} X(0, \dots, q+2) \right), \quad (21b)$$

$$P_2^- = \left(\prod_{q=0}^{s-3} C^a X(0, \dots, a) \right) CX(0, 1) X_0, \quad (21c)$$

where $a = s-q-1$ and $n_x = 2^s$. Here, $C^j X(q_0, \dots, q_j)$ is a multi-control NOT gate whereby the first q_0, \dots, q_{j-1} arguments are control qubits and the final q_j argument is the target. Additionally, $CX(q_{j-1}, q_j)$ is the CNOT gate with control on the q_{j-1} qubit and target on the q_j qubit, and X_0 is the NOT-gate applied to the 0th qubit. Note that the complexity of the P_2^+ and P_2^- matrices can be improved upon as discussed in [52].

The final component of (8) to decompose is the commutation matrix, which is given by

$$K^{(a,b)} = \prod_{r=0}^{n-1} \prod_{q=0}^{m-1} S(r+m-q-1, r+m-q), \quad (22)$$

where $a = 2^m, b = 2^n, S(i, j)$ is the SWAP gate between the i^{th} and j^{th} qubits. The circuit depth complexities for P_1, P_2^-, P_2^+ , and $K^{(a,b)}$ are all polylogarithmic and are discussed in Section VII.

VI. BLOCK ENCODING

The work in Section V provides us with a linear combination of non-unitary matrices for $L^{(e)}$. The next step towards generalizing the technique of [48] requires us to block encode each term of this linear combination. If the general form of the original linear combination is given

in (12), then we must block encode each L_l into a unitary matrix $U_l \in \mathbb{C}^{2\alpha n_t n_x^\alpha \times 2\alpha n_t n_x^\alpha}$ where $U_l = U_{l,1} U_{l,2}$ as discussed in [48]. For convenience, in the remainder of this section the subscript l is dropped.

As discussed in Section V, $L^{(e)}$ is split into three types of terms $L_1^{(e)}$, $L_{2a}^{(e)}$ and $L_{2b}^{(e)}$. Since both the $L_1^{(e)}$ and $L_{2a}^{(e)}$ terms were shown in Section V to be decomposed into purely elements from \mathbb{P} , they can be treated following [48]. In contrast, the $L_{2b}^{(e)}$ terms are decomposed into products of elements from \mathbb{P} with the permutation matrices introduced in Section V B. The remainder of this section will focus on demonstrating that the methods in [48] can be extended to block encode the $L_{2b}^{(e)}$ terms.

By evaluating (8) into (17b), we can see that the $L_{2b}^{(e)}$ terms have the general form

$$\begin{aligned} \mathcal{A} = & \left(\bigotimes_{k=0}^{Q_1-1} \rho_{r_k} \right) \\ & \otimes \left(\left(\rho_0^{\otimes \log n_x} \otimes K^{(n_x^l, n_x)} \right) \right. \\ & \left. \cdot \left(\mathcal{D}P \otimes I_{n_x}^{\otimes l} \right) \cdot K^{(n_x^2, n_x^l)} \right) \otimes I_{n_x}^{\otimes j-l-1}, \end{aligned} \quad (23)$$

where $\mathcal{A} \in \mathbb{C}^{\alpha n_t n_x^\alpha \times \alpha n_t n_x^\alpha}$, $\rho_{r_k} \in \mathbb{P}$, $r_k \in \{0, \dots, 4\}$, $P \in \{P^+, P^-\}$, \mathcal{D} is defined in (20), and $Q_1 = \log(\alpha n_t n_x^\alpha / n_x^{j+1})$.

Theorem 1. *One choice of unitary completion for (23) is given by*

$$\begin{aligned} \bar{\mathcal{A}} = & \left(\bigotimes_{k=0}^{Q_1-1} \bar{\rho}_{r_k} \right) \\ & \otimes \left(\left(\rho_4^{\otimes \log n_x} \otimes K^{(n_x^l, n_x)} \right) \right. \\ & \left. \cdot \left(P \otimes I_{n_x}^{\otimes l} \right) \cdot K^{(n_x^2, n_x^l)} \right) \otimes I_{n_x}^{\otimes j-l-1}, \end{aligned} \quad (24)$$

where $\bar{\rho}_k$ is defined in (1).

Proof. See Appendix E. \square

Theorem 1 shows that a simple procedure exists for each unitary completion of the $L_{2b}^{(e)}$ terms. Next, using this result we show that matrices of the form (23) have a simple block encoding.

Theorem 2. *For a matrix \mathcal{A} as defined in (23), the following relations are true:*

$$U := \begin{pmatrix} \mathcal{A}^c & \mathcal{A} \\ \mathcal{A} & \mathcal{A}^c \end{pmatrix} = U_1 U_2,$$

where we have

$$\begin{aligned} U_1 &:= \begin{pmatrix} I - \mathcal{A}\mathcal{A}^T & \mathcal{A}\mathcal{A}^T \\ \mathcal{A}\mathcal{A}^T & I - \mathcal{A}\mathcal{A}^T \end{pmatrix}, \\ U_2 &:= \begin{pmatrix} \bar{\mathcal{A}} & 0 \\ 0 & \mathcal{A} \end{pmatrix}. \end{aligned}$$

Moreover, both U_1 and U_2 are unitary matrices.

Proof. See Appendix F. \square

Theorem 2 demonstrates that the block encoded matrix U can be implemented by two simpler unitary operations. The following two theorems show that each of these unitary operations have polylogarithmic gate-depths.

Theorem 3. *For \mathcal{A} defined as in (23), the U_1 matrix given by Theorem 2 can be implemented with a single $C^q X$ gate, where $q \leq \log(\alpha n_t n_x^\alpha)$.*

Proof. First, observe that $\rho_{r_k} \rho_{r_k}^T \in \{\rho_0, \rho_3, \rho_4\}$ for $\rho_{r_k} \in \mathbb{P}$. Using this property and by evaluating (20) into (F1), it follows that $\mathcal{A}\mathcal{A}^T$ is composed solely of terms from the set $\{\rho_0, \rho_3, \rho_4\}$. Thus, $\mathcal{A}\mathcal{A}^T$ is a binary diagonal matrix exactly as in Theorem 3 of [48] and, therefore, their proof that U_1 can be implemented with a single multi-control gate is also applicable here. Following [48], the upper bound on q simply comes from the number of qubits required to implement \mathcal{A} , which in this case is $\log(\alpha n_t n_x^\alpha)$. \square

The explicit circuit implementation of the U_1 matrix is given in the proof of Theorem 3 in [48]. An important result of theirs is that the number of control qubits is equal to the number of $\rho_{r_k} \rho_{r_k}^T \in \mathbb{P} \setminus \{\rho_4\}$ terms in the $\mathcal{A}\mathcal{A}^T$ expansion. Next, we show that the U_2 circuit is also efficient.

Theorem 4. *For \mathcal{A} defined as in (23), the U_2 matrix given by Theorem 2 can be implemented with gate depth equal to the combined depths of P , $K^{(n_x^l, n_x)}$, and $K^{(n_x^2, n_x^l)}$ plus at most $\log(\alpha n_t n_x^{\alpha-2})$ Pauli- X gates.*

Proof. From the definition of U_2 and Theorem 1 we have,

$$\begin{aligned} U_2 &= \begin{pmatrix} \bar{\mathcal{A}} & 0 \\ 0 & \mathcal{A} \end{pmatrix} = \rho_4 \otimes \bar{\mathcal{A}} \\ &= \rho_4 \otimes \left(\bigotimes_{k=0}^{Q_1-1} \bar{\rho}_{r_k} \right) \\ &\quad \otimes \left(\left(\rho_4^{\otimes \log n_x} \otimes K^{(n_x^l, n_x)} \right) \right. \\ &\quad \left. \cdot \left(P \otimes I_{n_x}^{\otimes l} \right) \cdot K^{(n_x^2, n_x^l)} \right) \otimes I_{n_x}^{\otimes j-l-1}. \end{aligned}$$

So the U_2 complexity depends upon P , $K^{(n_x^l, n_x)}$, and $K^{(n_x^2, n_x^l)}$. Additionally, there are Q_1 tensor products

of $\bar{\rho}_{r_k}$ terms. From Theorem 1 it follows that $Q_1 = \log(\alpha n_t n_x^\alpha / n_x^{j+1})$, and since $\bar{\rho}_{r_k} \in \{I, X\}$, then there are at most $\log(\alpha n_t n_x^\alpha / n_x^{j+1})$ Pauli-X gates. This is maximized for $j = 1$, so we have at most $\log(\alpha n_t n_x^{\alpha-2})$ Pauli-X gates. \square

Theorems 1 - 4 demonstrate how to block encode the $L_{2b}^{(e)}$ terms with complexity that depends on the P , $K^{(n_x^l, n_x)}$, and $K^{(n_x^2, n_x^l)}$ matrices. In the next section, we show that the gate-depth complexities for the circuit implementations of these matrices is polylogarithmic, thereby demonstrating that U_2 is efficient.

VII. RESOURCE ESTIMATION

There are three types quantities relevant for resource estimation [53]: (1) the number of qubits, (2) the number of terms in the linear combination of $L^{(e)}$ (N_s from (12)), and (3) the Clifford (composed of Hadamard, phase, and CNOT gates) and T (aka $Z^{1/4}$) gate counts required to load each matrix in the decomposition. The number of qubits required is exactly $\log(\alpha n_t n_x^\alpha) + 1$ where the additional qubit is an ancillary qubit required for the block encoding strategy outlined in Section VI. The latter two estimates are summarized in Table I and described in more detail below.

The total number of terms can also be exactly calculated. From (13) and (16), $L^{(e)}$ is split into the $L_1^{(e)}$, $L_{2a}^{(e)}$ and $L_{2b}^{(e)}$ terms. Conveniently, $L_1^{(e)}$ is decomposed into exactly $\log n_t + 1$ terms as shown in (14). By combining (5a), (7), (17a) and (18) we can see that $L_{2a}^{(e)}$ has $(4 \log n_x + 6) \sum_{j=1}^{\alpha} j = \alpha(\alpha + 1)(2 \log n_x + 3)$ terms. Similarly, by combining (8), (17b) and (19) we can see that $L_{2b}^{(e)}$ has $4 \sum_{j=1}^{\alpha-1} j = 2\alpha(\alpha - 1)$ terms. By adding all three contributions together, the total number of terms in the decomposition of $L^{(e)}$ is exactly $\log n_t + 2\alpha(\alpha + 1) \log n_x + \alpha(5\alpha + 1) + 1$, which we say has complexity $\mathcal{O}(\log n_t + \alpha^2 \log n_x)$ number of terms assuming that $n_x = n_t$ and $2 \leq \alpha \ll n_x$.

Finally, to obtain an estimate of the Clifford and T gate counts, we require the following facts and assumptions (referred to as items):

1. A $C^q X$ gate can be implemented with $\mathcal{O}(q)$ Clifford and $\mathcal{O}(q)$ T-gates using one dirty ancilla [54].
2. An adjacent Toffoli gate is implemented with a constant number of Clifford (CNOT, H, Pauli or S) and T-gate [55].
3. An adjacent SWAP gate is implemented with three CNOT gates [56].
4. Assume that $n_t = n_x$.

Here, we estimate the Clifford and T gate count for an arbitrary term in our decomposition L_l , by estimating the resources required for its block encoding $U_l = U_{l,1} U_{l,2}$ as

described in Section VI. For the remainder of this section we will drop the l subscript and refer to these terms as L , U , U_1 and U_2 . Since U_1 can be implemented with a single $C^q X$ gate, as described in Section VI, its gate complexity scales like $\mathcal{O}(q)$ from item 1. The procedure to determine the value q is simply to count the number of operators from the set $\mathbb{P} \setminus \rho_4$ that appear in the term LL^T (see [48, 50] for a detailed explanation). Similarly, the procedure to determine U_2 is to obtain \bar{L} and to use the relation $U_2 = I \otimes \bar{L}$. Bringing these ideas together, as an example consider the term $L = \rho_0 \otimes \rho_1 \otimes \rho_2 \otimes \rho_3 \otimes \rho_4 \otimes P$ for an arbitrary permutation matrix P . From this we find that $LL^T = \rho_0 \otimes \rho_0 \otimes \rho_3 \otimes \rho_3 \otimes \rho_4 \otimes \rho_4$ and $\bar{L} = \rho_4 \otimes \sigma_0 \otimes \sigma_0 \otimes \rho_4 \otimes P$. Therefore, the associated U_1 matrix requires one $C^4 X$ gate and the associated U_2 circuit requires two NOT gates and the circuit for P .

This procedure, in conjunction with the items listed above, is applied to estimate the Clifford and T gate counts for each of the $L_1^{(e)}$, $L_{2a}^{(e)}$ and $L_{2b}^{(e)}$ terms as summarized in Table I. To provide a concrete example about how these estimates were formed, we consider the most expensive $L_{2b}^{(e)}$ term. This term comes about by evaluating (8) and (19) into (17b) and choosing $j = \alpha - 1$, $l = \alpha - 2$, the $\rho_0^{\otimes \log n_t}$ term from (17b), and the F^+ component from (19). The resulting L , \bar{L} and LL^T terms are provided in the box of Figure 4. The U_1 term requires a single $C^q X$ gate where $q = \log \alpha n_t n_x$ since LL^T has as many operators from the set $\mathbb{P} \setminus \rho_4$. Next, by looking at the \bar{L} term it follows that the U_2 circuit requires a single NOT gate plus the circuits for $K^{(n_x^{\alpha-2}, n_x)}$, P_2^+ , P_1 and $K^{(n_x^2, n_x^{\alpha-2})}$. By invoking items items 1 to 3 and from (21a), (21b) and (22), these circuits require $\mathcal{O}(\alpha(\log n_x)^2)$ Clifford gates and $\mathcal{O}((\log n_x)^2)$ T gates, as appear in Table I.

VIII. NUMERICAL SIMULATIONS

In this section we implement our decomposition strategy to (i) generate circuits that load the Carleman linearized 1D Burgers' equation, and (ii) use these circuits to obtain a solution to the linear system using the VQLS method. We start with the nonlinear PDE provided in (2) with the following parameter settings: $n_t = 4$, $n_x = 4$, $\Delta t = 0.25$ s, $\Delta x = 2\pi/(n_x - 1)$ m, $\nu = 1.0$ m²s⁻¹, and a Gaussian distribution for the initial condition given by $u(x, 0) = (\sqrt{2\pi\sigma^2})^{-1} e^{-(x-\mu)^2/(2\sigma^2)}$ with $\sigma = 0.5$ and $\mu = \pi$. The Carleman linearization is then applied with a truncation order of $\alpha = 2$ resulting in an equation of the form (10) with $L^{(e)} \in \mathbb{C}^{128 \times 128}$.

Next, we apply the decomposition strategy described in Section V. Here, we find that $L^{(e)}$ may be decomposed into a linear combination of 73 non-unitary matrices that are then individually block encoded using the strategy described in Section VI. For a point of reference, a decomposition of the same matrix using a linear combination of tensor products of Pauli matrices requires 1,142

| Cost to Encode Carleman Linearized 1D Burgers' Equation | | | | | |
|---|---------------------------|------------------------------|--------------------|------------------------------|--------------------------------------|
| Term | Clifford Count (Min, Max) | | T Count (Min, Max) | | No. of Terms (Exact) |
| $L_1^{(e)}$ | 1 | $\log n_t$ | 0 | $\log n_t$ | $\log n_t + 1$ |
| $L_{2a}^{(e)}$ | $\log \alpha$ | $\log \alpha n_t n_x^\alpha$ | $\log \alpha$ | $\log \alpha n_t n_x^\alpha$ | $\alpha(\alpha + 1)(2 \log n_x + 3)$ |
| $L_{2b}^{(e)}$ | $\log \alpha n_x$ | $\alpha(\log n_x)^2$ | $\log \alpha n_x$ | $(\log n_x)^2$ | $2\alpha(\alpha - 1)$ |

TABLE I: A resource estimate of the Clifford and T-gate counts, and number of terms for the zero padded Carleman linearized 1D Burgers' equation from (10). The $L_1^{(e)}$ term comes from (14), the $L_{2a}^{(e)}$ from (17a), and the $L_{2b}^{(e)}$ from (17b). Since each term is split into many terms of varying cost, we provide the minimum and maximum Clifford and T-gate counts for each to provide a range. The Clifford and T-gate count columns use big O notation, though the $\mathcal{O}(\cdot)$ has been dropped for convenience. The Number of Terms column is an exact count.

terms. Using our approach, there are three types of circuits stemming from the terms $L_1^{(e)}$, $L_{2a}^{(e)}$ and $L_{2b}^{(e)}$, which are (14), (17a) and (17b) respectively. A characteristic example for each of these three types of circuits are given in Figures 2 to 4, respectively, demonstrating that our method provides complete constructions. Circuits in the forms of Figures 2 to 4 are used to generate all of the 73 aforementioned terms in the linear combination of $L^{(e)}$.

Next, we combine our approach with the VQLS algorithm from [12] to obtain a solution to the linear system in (10) for this specific setup. The VQLS method is a variational approach whereby an ansatz ($V(\vec{\theta})$) with variational parameters ($\vec{\theta}$) is used to approximate the true solution ($\vec{Y}^{(e)}$) by searching the parameter space to find the optimal parameters ($\vec{\theta}_{\text{opt}}$) such that $V(\vec{\theta}_{\text{opt}})|0\rangle \approx \vec{Y}^{(e)}$. To do this, the quantum computer is tasked with calculating the classically intractable expectation values that are then passed to a classical computer to (i) compute a cost function, and (ii) update the variational parameters using an optimization routine. Given the updated variational parameters, the quantum computer recomputes the expectation values and again passes the information back to the classical computer to repeat (i) and (ii). This back-and-forth process is repeated until the cost function reaches a predefined minimum at which point $V(\vec{\theta}_{\text{opt}})$ is obtained.

To implement the VQLS routine one requires a cost function, ansatz, and an optimization routine. First, to avoid the barren plateau phenomena [58], we have elected to use the local cost function outlined in [12], which, if we consider the decomposition from (12), is written as

$$C(\vec{\theta}) = \frac{1}{2} \left(1 - \frac{1}{n} \frac{\sum_{k=0}^{n-1} \sum_{l,l'=0}^{N_s-1} c_l c_{l'}^* \delta_{l,l'}^k}{\sum_{l,l'=0}^{N_s-1} c_l c_{l'}^* \beta_{l,l'}} \right)$$

$$\delta_{l,l'}^k = \langle V(\vec{\theta}) | L_l^\dagger U_b Z_k U_b^\dagger L_l | V(\vec{\theta}) \rangle$$

$$\beta_{l,l'} = \langle V(\vec{\theta}) | L_l^\dagger L_l | V(\vec{\theta}) \rangle,$$

where n is the number of qubits, $N_s = 73$ for the pa-

rameters selected in this section, the coefficients c_l come from (12), $U_b|0\rangle = \vec{B}^{(e)}$ loads the RHS of (10), and Z_k is the Pauli-Z matrix applied on the k^{th} qubit. Next, for our ansatz we use Circuit 18 from [59] and reproduced in Figure 5, which is hardware efficient with decent expressibility and entangling capabilities. Since the dimension of this test problem is small, we need only three ansatz layers yielding $3n = 21$ total variational parameters for number of qubits $n = \log(\alpha n_t n_x^\alpha)$. Finally, we use the conjugate gradient optimizer available in IBM Qiskit's software package `qiskit_algorithms.optimizers` with a tolerance setting of 10^{-3} . The conjugate gradient optimizer was used because it was found to perform the best among twelve commonly used optimizers for idealized (noiseless) settings [60] such as the one used here. It is important to note that there are better choices for noisy settings.

Bringing everything together, the VQLS solution to the Carleman linearized 1D Burgers' equation using our novel decomposition strategy is shown in Figure 6. For validation, we compare our quantum solution to a classical solution whereby we have solved exactly the same linear system, but have instead used the `python` function `numpy.linalg.solve` to obtain a solution. A visual comparison shows that the quantum solution validates well to the classical solution, thereby demonstrating that our decomposition strategy is capable of producing accurate results.

IX. DISCUSSION AND CONCLUSIONS

In this work, we solve the decomposition problem for the 1D Carleman linearized Burgers' equation. The key insights introduced in this study are two-fold: (1) to embed the original Carleman system into an even larger system of equations, and (2) to extend the methods introduced in [48] to include products of elements from \mathbb{P} with specific unitary matrices. The advantage gained from these insights is that the larger system can be decomposed into a linear combination of $\mathcal{O}(\log n_t + \alpha^2 \log n_x)$

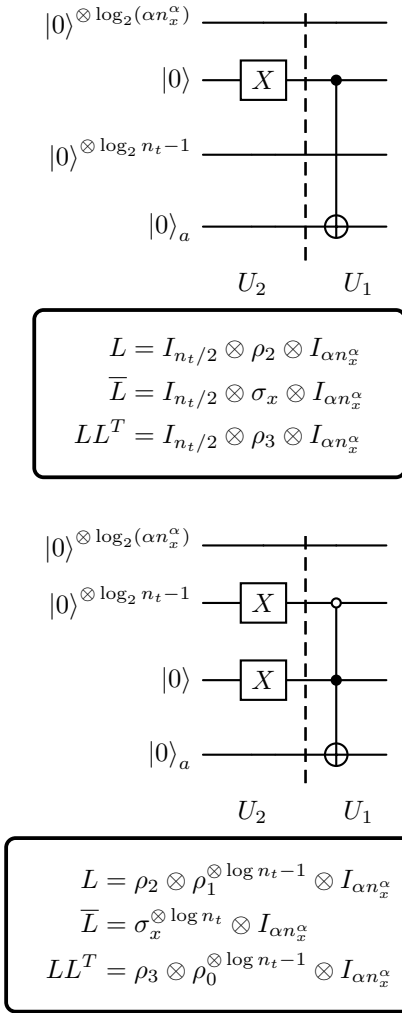


FIG. 2: Circuits for the two nontrivial block encoded $L_1^{(e)}$ terms from (14) are given. The $|0\rangle_a$ wire is a single ancillary qubit required for the block encoding described in Section VI. A control operation or a single qubit gate on a multi-qubit register should be interpreted as the respective operation being applied to each individual wire within that register. The vertical dashed line separates the U_1 from the U_2 component corresponding to the block encoding discussed in Section VI. The equations below the circuits are: the term to block encode (L), its completion (\bar{L}) which is necessary to construct $U_2 = I \otimes \bar{L}$, and LL^T which is used to construct U_1 using the approach outlined in [48]. The bottom circuit is formed by choosing $j = 2$ in the summation. Circuits drawn using [57].

terms, whereas the original has no known polylogarithmic decomposition. While these terms are non-unitary, they can be efficiently block encoded into unitary matrices, and therefore used in a QLSA. As an example, we use the VQLS where we found that the upper bounds for the Clifford and T gate counts are $\mathcal{O}(\alpha(\log n_x)^2)$ and $\mathcal{O}((\log n_x)^2)$ respectively. Together, these polylogarithmic

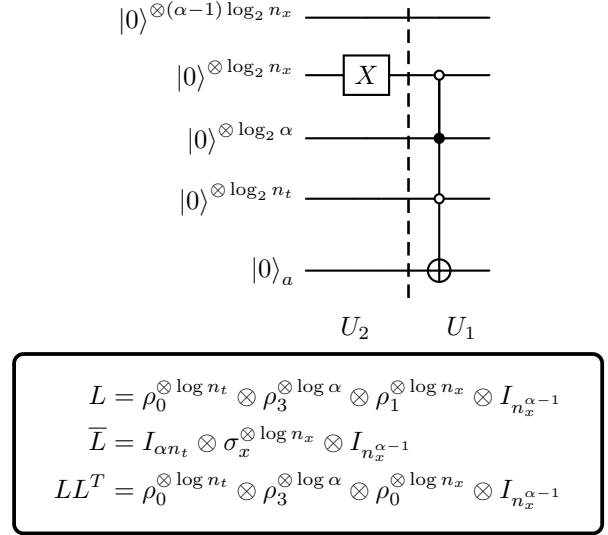


FIG. 3: Same as Figure 2, except for the $L_{2a}^{(e)}$ term where we have evaluated both (5a) and (18) into (17a) and chosen $j = \alpha$, $l = 0$, the $\rho_0^{\otimes \log n_t}$ term from (17a), and the $\rho_1^{\otimes s}$ term ($s = \log n_x$) from (18). The circuit will take a similar form for other values of j , l and if other terms from (18) are used. Note that the circuit has the same width as those from Figure 2.

mic scalings suggest that it may be possible to exponentially increase the spatial and temporal grid sizes in CFD and NWP models. That being said, whether an exponential increase is possible is still an open question and there are still major challenges that must be solved.

One such challenge with the Carleman linearized Burgers' (or Navier-Stokes) equation is that, for strongly nonlinear interactions, it may not be possible to efficiently find accurate solutions, as put forth by [16]. However, this may be a case of learning through experiment since their empirical results do differ from their analytical results. One way to completely circumvent the strong nonlinearity issue is to apply the Carleman linearization method to the Lattice-Boltzman equation (LBE) rather than the Navier-Stokes [18]. The advantage being that the LBE is inherently weakly nonlinear provided that the Mach number is small. It is therefore important to note that while the present study focused on the 1D Burgers' equation, the zero padding method introduced here can also be applied to the LBE. In fact, a related embedding technique was introduced in the encoding oracles in [29]. The work presented here therefore fits well into the quantum algorithm literature by contributing a generalizable method useful for different approaches.

Another such challenge is related to the data read-out problem, whereby quantum advantage may be lost when extracting exponentially small probability amplitudes from the state vector. In Liu *et al.* [16], they find that for dissipative systems “we must have a suitable

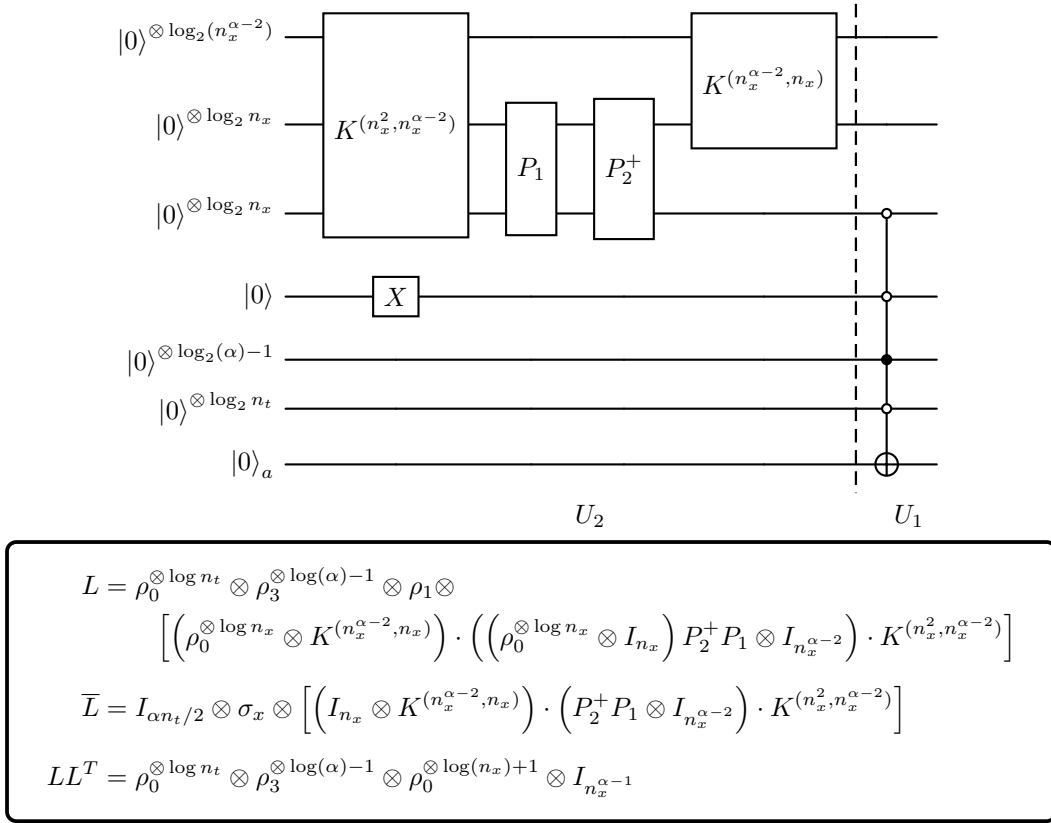


FIG. 4: Same as Figure 2, except for the $L_{2b}^{(e)}$ term where we have evaluated (8) and (19) into (17b) and chosen $j = \alpha - 1$, $l = \alpha - 2$, the $\rho_0^{\otimes \log n_t}$ term from (17b), and the F^+ component from (19). The circuit will take a similar form for other values of j , l and if the F^- term is used instead of F^+ . The circuits for P_1 and P_2^+ are given in (21a) and (21b) respectively, and the circuits for the commutation matrices $K^{(a,b)}$ are given in (22). Note that the circuit has the same width as those from Figures 2 and 3.

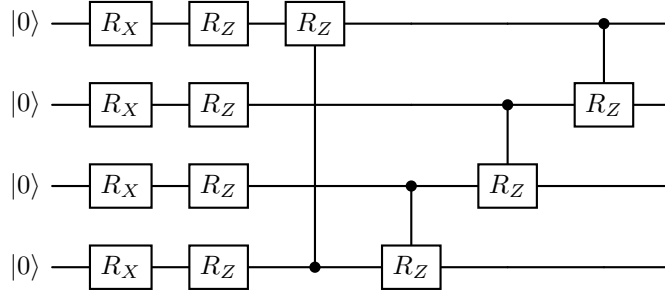


FIG. 5: A single layer of the ansatz used for the VQLS routine taken from Circuit 18 from [59].

initial condition and terminal time such that the final state is not exponentially smaller than the initial state.” The reasoning comes about because if the final solution is exponentially smaller than the initial state, then reading the probability amplitudes of the final state could take an exponential number of final state preparations. If instead we consider a dissipative system with a forcing term, then the final state is not necessarily exponentially smaller than the initial state, and therefore readout can

be efficient. Given that, quantum advantage for the homogeneous case may not be possible if the terminal time t_{final} is too large such that the amplitude of the solution at t_{final} is exponentially smaller than that of the initial condition. Therefore, t_{final} will depend upon both the initial state and the diffusion coefficient ν , and must be chosen carefully to ensure that the final solution is not exponentially smaller than the initial state.

Finally, an important limitation of this work is that

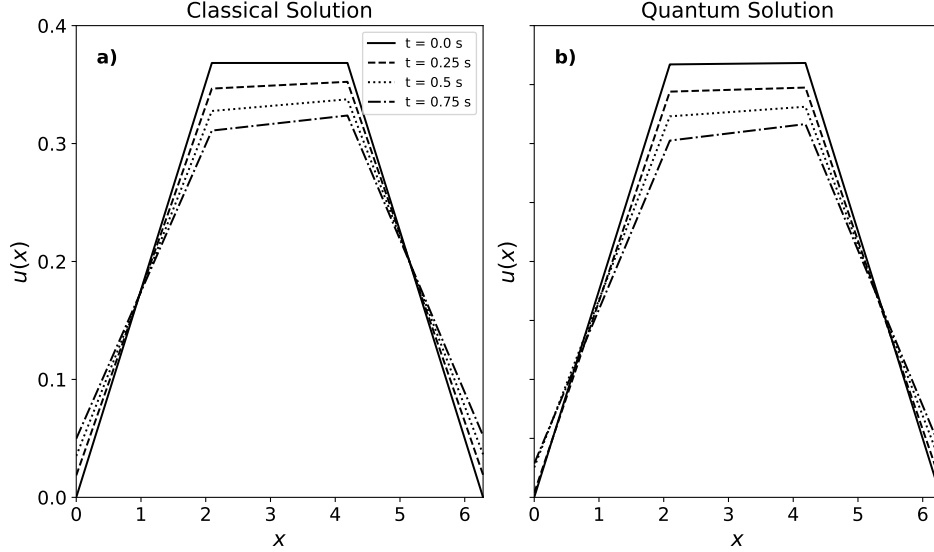


FIG. 6: Solutions to the Carleman linearized 1D Burgers equation from (10) using (a) a classical linear systems solver, and (b) our decomposition approach combined with VQLS [12]. The initial condition is the solid black line and the evolution at integer multiples of 0.25 s is provided in the dashed and dotted lines.

we make no effort to transpile our circuits since that is a device specific process. While our decompositions do achieve the desirable polylogarithmic circuit depth complexity, we implicitly assume an all-to-all connectivity for the topology. A different topology will introduce more overhead and, since the overhead is device specific, we cannot make general remarks on how this will impact our circuit depth complexities. That being said, the circuit depths reported here are a starting point and are certainly not optimal. In fact, there are known improvements to at least two of the circuits used, that are the incrementer [52] and the decomposition of the $C^j X$ gates

[54]. So, while the transpilation of our circuits onto real hardware will incur some overhead, there is also reason to believe that we can even potentially improve upon the circuit depths reported here.

ACKNOWLEDGEMENTS

We gratefully acknowledge the support NRL Base Program PE 0601153N. Furthermore, we are thankful for the stimulating discussions with Dr. Arzhang Angoshtari.

Appendix A: Example of the Quaternary Mappings

Table II lists some arbitrary examples of the quaternary mapping method introduced in Section IV. The purpose of these terms is to place the $A_j^{(e),j}$ and $A_{j+1}^{(e),j}$ terms in (9) in their appropriate positions along the diagonal and super-diagonal respectively.

Appendix B: Derivation for $A_{j+1}^{(e),j}$ (8)

Here, we derive the $A_{j+1}^{(e),j}$ equation for $j = \{1, \dots, \alpha - 1\}$. First, we expand (5b) using the property $A \otimes B = K^{(r,m)} \cdot (B \otimes A) \cdot K^{(n,q)}$ where $A \in \mathbb{C}^{r \times q}$, $B \in \mathbb{C}^{m \times n}$, and $K^{(a,b)} \in \mathbb{C}^{ab \times ab}$ is the commutation matrix [61, 62]. Using the definition of A_{j+1}^j from (5b), this gives

$$\begin{aligned}
 A_{j+1}^j &= \sum_{l=0}^{j-1} I_{n_x}^{\otimes l} \otimes F_2 \otimes I_{n_x}^{\otimes j-l-1} \\
 &= \sum_{l=0}^{j-1} \left(K^{(n_x^l, n_x)} \cdot (F_2 \otimes I_{n_x}^{\otimes l}) \cdot K^{(n_x^2, n_x^l)} \right) \otimes I_{n_x}^{\otimes j-l-1}.
 \end{aligned} \tag{B1}$$

| α | i | j | $b_\alpha(i)$ | $b_\alpha(j)$ | $f(b_\alpha(i), b_\alpha(j))$ | $\rho_{f_{K-1}\dots f_0}$ |
|----------|-----|-----|---------------|---------------|-------------------------------|--|
| 2 | 0 | 0 | 0 | 0 | 0 | ρ_0 |
| 2 | 0 | 1 | 0 | 1 | 1 | ρ_1 |
| 4 | 0 | 1 | 00 | 01 | 01 | $\rho_0 \otimes \rho_1$ |
| 4 | 2 | 3 | 10 | 11 | 31 | $\rho_3 \otimes \rho_1$ |
| 8 | 1 | 5 | 001 | 101 | 103 | $\rho_1 \otimes \rho_0 \otimes \rho_3$ |
| 8 | 6 | 7 | 110 | 111 | 331 | $\rho_3 \otimes \rho_3 \otimes \rho_1$ |

TABLE II: Some arbitrary examples for the quaternary mapping method discussed in Section IV. Here, α is the truncation order, i, j are matrix element indices, $b_\alpha(k)$ is the decimal to binary mapping function of bitstring length $\log \alpha$, $f(b_\alpha(i), b_\alpha(j))$ maps the binary values to their respective quaternary values, and $\rho_{f_{K-1}\dots f_0}$ are the full products using the quaternary bitstrings.

Next, we evaluate (B1) into (8) to obtain

$$\begin{aligned}
A_{j+1}^{(e),j} &:= \begin{pmatrix} A_{j+1}^j & 0_{n_x^j \times (n_x^\alpha - n_x^{j+1})} \\ 0_{(n_x^\alpha - n_x^j) \times n_x^{j+1}} & 0_{(n_x^\alpha - n_x^j) \times (n_x^\alpha - n_x^{j+1})} \end{pmatrix} \\
&= \begin{pmatrix} \left(\sum_{l=0}^{j-1} \left(K^{(n_x^l, n_x)} \cdot (F_2 \otimes I_{n_x}^{\otimes l}) \cdot K^{(n_x^2, n_x^l)} \right) \otimes I_{n_x}^{\otimes j-l-1} & 0_{n_x^j \times (n_x^\alpha - n_x^{j+1})} \right) \\ & 0_{(n_x^\alpha - n_x^j) \times n_x^{j+1}} & 0_{(n_x^\alpha - n_x^j) \times (n_x^\alpha - n_x^{j+1})} \end{pmatrix} \\
&= \sum_{l=0}^{j-1} \begin{pmatrix} \left(K^{(n_x^l, n_x)} \cdot (F_2 \otimes I_{n_x}^{\otimes l}) \cdot K^{(n_x^2, n_x^l)} \right) \otimes I_{n_x}^{\otimes j-l-1} & 0_{n_x^j \times (n_x^\alpha - n_x^{j+1})} \\ & 0_{(n_x^\alpha - n_x^j) \times n_x^{j+1}} & 0_{(n_x^\alpha - n_x^j) \times (n_x^\alpha - n_x^{j+1})} \end{pmatrix} \quad (\text{B2}) \\
&= \sum_{l=0}^{j-1} \begin{pmatrix} \left(K^{(n_x^l, n_x)} \cdot (F_2 \otimes I_{n_x}^{\otimes l}) \cdot K^{(n_x^2, n_x^l)} \right) & 0_{n_x^{l+1} \times (n_x^\alpha - j + l + 1 - n_x^{l+2})} \\ & 0_{(n_x^\alpha - j + l + 1 - n_x^{l+1}) \times n_x^{l+2}} & 0_{(n_x^\alpha - j + l + 1 - n_x^{l+1}) \times (n_x^\alpha - j + l + 1 - n_x^{l+2})} \end{pmatrix} \otimes I_{n_x}^{\otimes j-l-1} \\
&= \rho_0^{\otimes \log(n_x^\alpha - j - 1)} \otimes \sum_{l=0}^{j-1} \begin{pmatrix} K^{(n_x^l, n_x)} \cdot (F_2 \otimes I_{n_x}^{\otimes l}) \cdot K^{(n_x^2, n_x^l)} \\ & 0_{(n_x^{l+2} - n_x^{l+1}) \times n_x^{l+2}} \end{pmatrix} \otimes I_{n_x}^{\otimes j-l-1}.
\end{aligned}$$

Next, we simplify the matrix product terms by

$$\begin{aligned}
&\begin{pmatrix} K^{(n_x^l, n_x)} \cdot (F_2 \otimes I_{n_x}^{\otimes l}) \cdot K^{(n_x^2, n_x^l)} \\ & 0_{(n_x^{l+2} - n_x^{l+1}) \times n_x^{l+2}} \end{pmatrix} = \begin{pmatrix} K^{(n_x^l, n_x)} \cdot (F_2 \otimes I_{n_x}^{\otimes l}) \\ & 0_{(n_x^{l+2} - n_x^{l+1}) \times n_x^{l+2}} \end{pmatrix} \cdot K^{(n_x^2, n_x^l)} \\
&= \begin{pmatrix} K^{(n_x^l, n_x)} & 0_{n_x^{l+1} \times (n_x^{l+2} - n_x^{l+1})} \\ 0_{(n_x^{l+2} - n_x^{l+1}) \times n_x^{l+1}} & 0_{(n_x^{l+2} - n_x^{l+1}) \times (n_x^{l+2} - n_x^{l+1})} \end{pmatrix} \cdot \begin{pmatrix} F_2 \otimes I_{n_x}^{\otimes l} \\ & 0_{(n_x^{l+2} - n_x^{l+1}) \times n_x^{l+2}} \end{pmatrix} \cdot K^{(n_x^2, n_x^l)} \quad (\text{B3}) \\
&= \left(\rho_0^{\otimes \log n_x} \otimes K^{(n_x^l, n_x)} \right) \cdot \left(\begin{pmatrix} F_2 \\ & 0_{(n_x^2 - n_x) \times n_x^2} \end{pmatrix} \otimes I_{n_x}^{\otimes l} \right) \cdot K^{(n_x^2, n_x^l)}.
\end{aligned}$$

Finally, evaluate (B3) into (B2) to give the full expression

$$\begin{aligned}
A_{j+1}^{(e),j} &= \rho_0^{\otimes \log(n_x^\alpha - j - 1)} \\
&\otimes \sum_{l=0}^{j-1} \left[\left(\rho_0^{\otimes \log n_x} \otimes K^{(n_x^l, n_x)} \right) \cdot \left(\begin{pmatrix} F_2 \\ & 0_{(n_x^2 - n_x) \times n_x^2} \end{pmatrix} \otimes I_{n_x}^{\otimes l} \right) \cdot K^{(n_x^2, n_x^l)} \right] \otimes I_{n_x}^{\otimes j-l-1}.
\end{aligned}$$

Appendix C: Example Case: $n_x = 4$

For $n_x = 4$ we have

$$F_2^+ = \begin{pmatrix} 0 & 1 & 0 & 0 & 0 & 0 & 0 & 0 & 0 & 0 & 0 & 0 & 0 & 0 & 0 & 0 \\ 0 & 0 & 0 & 0 & 0 & 0 & 1 & 0 & 0 & 0 & 0 & 0 & 0 & 0 & 0 & 0 \\ 0 & 0 & 0 & 0 & 0 & 0 & 0 & 0 & 0 & 0 & 0 & 1 & 0 & 0 & 0 & 0 \\ 0 & 0 & 0 & 0 & 0 & 0 & 0 & 0 & 0 & 0 & 0 & 0 & 1 & 0 & 0 & 0 \end{pmatrix}, \quad (\text{C1a})$$

$$F_2^- = \begin{pmatrix} 0 & 0 & 0 & 1 & 0 & 0 & 0 & 0 & 0 & 0 & 0 & 0 & 0 & 0 & 0 & 0 \\ 0 & 0 & 0 & 0 & 1 & 0 & 0 & 0 & 0 & 0 & 0 & 0 & 0 & 0 & 0 & 0 \\ 0 & 0 & 0 & 0 & 0 & 0 & 0 & 0 & 0 & 1 & 0 & 0 & 0 & 0 & 0 & 0 \\ 0 & 0 & 0 & 0 & 0 & 0 & 0 & 0 & 0 & 0 & 0 & 0 & 0 & 1 & 0 & 0 \end{pmatrix}, \quad (\text{C1b})$$

where $F_2 = -(F_2^+ - F_2^-)/(2\Delta x)$. Therefore, the full matrix is given by

$$\begin{pmatrix} F_2 \\ 0_{(n_x^2 - n_x) \times n_x^2} \end{pmatrix} = \frac{-1}{2\Delta x} \begin{pmatrix} 0 & 1 & 0 & -1 & 0 & 0 & 0 & 0 & 0 & 0 & 0 & 0 & 0 & 0 & 0 & 0 \\ 0 & 0 & 0 & 0 & -1 & 0 & 1 & 0 & 0 & 0 & 0 & 0 & 0 & 0 & 0 & 0 \\ 0 & 0 & 0 & 0 & 0 & 0 & 0 & 0 & 0 & -1 & 0 & 1 & 0 & 0 & 0 & 0 \\ 0 & 0 & 0 & 0 & 0 & 0 & 0 & 0 & 0 & 0 & 0 & 1 & 0 & -1 & 0 & 0 \\ \hline 0 & 0 & 0 & 0 & 0 & 0 & 0 & 0 & 0 & 0 & 0 & 0 & 0 & 0 & 0 & 0 \\ 0 & 0 & 0 & 0 & 0 & 0 & 0 & 0 & 0 & 0 & 0 & 0 & 0 & 0 & 0 & 0 \\ 0 & 0 & 0 & 0 & 0 & 0 & 0 & 0 & 0 & 0 & 0 & 0 & 0 & 0 & 0 & 0 \\ 0 & 0 & 0 & 0 & 0 & 0 & 0 & 0 & 0 & 0 & 0 & 0 & 0 & 0 & 0 & 0 \\ 0 & 0 & 0 & 0 & 0 & 0 & 0 & 0 & 0 & 0 & 0 & 0 & 0 & 0 & 0 & 0 \\ 0 & 0 & 0 & 0 & 0 & 0 & 0 & 0 & 0 & 0 & 0 & 0 & 0 & 0 & 0 & 0 \\ 0 & 0 & 0 & 0 & 0 & 0 & 0 & 0 & 0 & 0 & 0 & 0 & 0 & 0 & 0 & 0 \\ 0 & 0 & 0 & 0 & 0 & 0 & 0 & 0 & 0 & 0 & 0 & 0 & 0 & 0 & 0 & 0 \\ 0 & 0 & 0 & 0 & 0 & 0 & 0 & 0 & 0 & 0 & 0 & 0 & 0 & 0 & 0 & 0 \\ 0 & 0 & 0 & 0 & 0 & 0 & 0 & 0 & 0 & 0 & 0 & 0 & 0 & 0 & 0 & 0 \\ 0 & 0 & 0 & 0 & 0 & 0 & 0 & 0 & 0 & 0 & 0 & 0 & 0 & 0 & 0 & 0 \\ 0 & 0 & 0 & 0 & 0 & 0 & 0 & 0 & 0 & 0 & 0 & 0 & 0 & 0 & 0 & 0 \end{pmatrix}.$$

Appendix D: Derivation of the Permutation Matrices: P_1, P_2^+ , and P_2^-

Figure 7 shows an example of how to create the $P^+ = P_2^+ P_1$ matrix for the $n_x = 4$ case (a similar procedure exists for P^-). The P_1 operation is straightforward to implement using the $\times(n_x + 1) \pmod{n_x^2}$ modular multiplication circuit given in (21a). Since $n_x + 1$ is odd, [63] provides a general implementation of the necessary modular multiplication circuit. However, we can considerably reduce the complexity of their circuit for our needs since the bottom $n_x^2 - n_x$ rows are non-unique. The only limitation of these latter rows, represented by C_2 in Figure 7, is that they must form a unitary complement to the first n_x rows, as discussed in Section V.

Next, the P_2^+ operation from (21b) increments each non-zero element forward by one. This is straightforward for each element except the $(n_x - 1, n_x^2 - 1)^{\text{th}}$ element, which must be carried over. Conveniently, we can also simultaneously satisfy the periodic boundary condition if carried over to the $(n_x - 1, n_x^2 - n_x)^{\text{th}}$ element. This type of carryover is achieved by applying the incremter on the first $\log n_x$ -qubits. Note that while there are many different incremter circuits as discussed in [52], we have chosen the multi-control NOT incremter simply as a starting point to be improved upon later.

Appendix E: Proof for Theorem 1

Proof. Here we prove that the unitary completion of \mathcal{A} , as defined in (23), is $\overline{\mathcal{A}}$, as defined in (24). As a consequence of Definition 1, if $\overline{\mathcal{A}}$ is the unitary completion to \mathcal{A} , then U is unitary where

$$U = \begin{pmatrix} \mathcal{A}^c & \mathcal{A} \\ \mathcal{A} & \mathcal{A}^c \end{pmatrix}.$$

$$\begin{array}{c}
\text{a) } \left(\begin{array}{cccccccccccccccc}
1 & 0 & 0 & 0 & 0 & 0 & 0 & 0 & 0 & 0 & 0 & 0 & 0 & 0 & 0 \\
0 & 1 & 0 & 0 & 0 & 0 & 0 & 0 & 0 & 0 & 0 & 0 & 0 & 0 & 0 \\
0 & 0 & 1 & 0 & 0 & 0 & 0 & 0 & 0 & 0 & 0 & 0 & 0 & 0 & 0 \\
0 & 0 & 0 & 1 & 0 & 0 & 0 & 0 & 0 & 0 & 0 & 0 & 0 & 0 & 0
\end{array} \right) \left. \vphantom{\begin{array}{c} \text{a) } \\ C_1 \end{array}} \right\} n_x = 4 \text{ rows} \\
\underbrace{\hspace{10em}}_{C_1 \in \mathbb{C}^{(n_x^2 - n_x) \times n_x^2}} \\
\text{Apply } P_1 \downarrow \begin{array}{l} \text{Space the first } n_x \\ \text{rows by } n_x + 1 \end{array} \\
\text{b) } \left(\begin{array}{cccccccccccccccc}
1 & 0 & 0 & 0 & 0 & 0 & 0 & 0 & 0 & 0 & 0 & 0 & 0 & 0 & 0 \\
0 & 0 & 0 & 0 & 0 & 1 & 0 & 0 & 0 & 0 & 0 & 0 & 0 & 0 & 0 \\
0 & 0 & 0 & 0 & 0 & 0 & 0 & 0 & 0 & 0 & 1 & 0 & 0 & 0 & 0 \\
0 & 0 & 0 & 0 & 0 & 0 & 0 & 0 & 0 & 0 & 0 & 0 & 0 & 0 & 1
\end{array} \right) \\
\underbrace{\hspace{10em}}_{C_2 \in \mathbb{C}^{(n_x^2 - n_x) \times n_x^2}} \\
\text{Apply } P_2^+ \downarrow \begin{array}{l} \text{Increment by 1} \\ \text{with limited carryover} \end{array} \\
\text{c) } \left(\begin{array}{cccccccccccccccc}
0 \rightarrow 1 & 0 & 0 & 0 & 0 & 0 & 0 & 0 & 0 & 0 & 0 & 0 & 0 & 0 & 0 \\
0 & 0 & 0 & 0 & 0 & 0 \rightarrow 1 & 0 & 0 & 0 & 0 & 0 & 0 & 0 & 0 & 0 \\
0 & 0 & 0 & 0 & 0 & 0 & 0 & 0 & 0 & 0 & 0 \rightarrow 1 & 0 & 0 & 0 & 0 \\
0 & 0 & 0 & 0 & 0 & 0 & 0 & 0 & 0 & 0 & 0 & 0 & 1 & 0 & 0
\end{array} \right) \\
\underbrace{\hspace{10em}}_{C_3 \in \mathbb{C}^{(n_x^2 - n_x) \times n_x^2}} \quad \text{Carryover}
\end{array}$$

FIG. 7: Operations to create the P^+ matrix for the $n_x = 4$ case. The P_1 matrix performs the $\times(n_x + 1) \pmod{n_x^2}$ modular multiplication to transform (a) the identity matrix into (b) an intermediary matrix where the first n_x non-zero elements are spaced by $n_x + 1$. Note that the C_1 matrix is the lower $n_x^2 - n_x$ portion of the identity matrix in (a), and that the C_2 matrix is a non-unique unitary complement to the upper $n_x \times n_x^2$ elements in (b). Next, the P_2^+ matrix increments each non-zero element by one with limited carryover to transform the intermediary matrix into (c) the P^+ matrix. Once again, the C_3 matrix is a non-unique unitary complement to the upper $n_x \times n_x^2$ elements. There is an analogous transformation to prepare P^- .

Therefore, to prove that $\overline{\mathcal{A}}$ is the unitary completion to \mathcal{A} , it is sufficient to show that U is unitary. Since all of the matrices used in our particular decomposition are real, the conjugate transpose is equivalent to the transpose. Therefore, we start with

$$\begin{aligned}
UU^T &= (I \otimes \mathcal{A}^c + \sigma_0 \otimes \mathcal{A})(I \otimes \mathcal{A}^{cT} + \sigma_0 \otimes \mathcal{A}^T) \\
&= I \otimes \mathcal{A}^c \mathcal{A}^{cT} + \sigma_0 \otimes \mathcal{A}^c \mathcal{A}^T + \sigma_0 \otimes \mathcal{A} \mathcal{A}^{cT} + I \otimes \mathcal{A} \mathcal{A}^T.
\end{aligned} \tag{E1}$$

From Definition 1, the first term can be expanded using

$$\mathcal{A}^c \mathcal{A}^{cT} = (\overline{\mathcal{A}} - \mathcal{A})(\overline{\mathcal{A}}^T - \mathcal{A}^T), \tag{E2}$$

where

$$\begin{aligned}
\overline{\mathcal{A}} \overline{\mathcal{A}}^T &= \left(\bigotimes_{k=0}^{Q_1-1} \overline{\rho}_{r_k} \overline{\rho}_{r_k}^T \right) \otimes I_{n_x}^{\otimes j+1}, \\
\overline{\mathcal{A}} \mathcal{A}^T &= \left(\bigotimes_{k=0}^{Q_1-1} \overline{\rho}_{r_k} \rho_{r_k}^T \right) \otimes \mathcal{D} \otimes I_{n_x}^{\otimes j-1}, \\
\mathcal{A} \overline{\mathcal{A}}^T &= \left(\bigotimes_{k=0}^{Q_1-1} \rho_{r_k} \overline{\rho}_{r_k}^T \right) \otimes \mathcal{D} \otimes I_{n_x}^{\otimes j-1}, \\
\mathcal{A} \mathcal{A}^T &= \left(\bigotimes_{k=0}^{Q_1-1} \rho_{r_k} \rho_{r_k}^T \right) \otimes \mathcal{D} \otimes I_{n_x}^{\otimes j-1},
\end{aligned}$$

| | $\rho_{r_k} = \rho_0$ | $\rho_{r_k} = \rho_1$ | $\rho_{r_k} = \rho_2$ | $\rho_{r_k} = \rho_3$ |
|-----------------------------------|----------------------------|------------------------------|-------------------------------------|----------------------------|
| $\bar{\rho}_{r_k} \rho_{r_k}^T =$ | $\rho_4 \rho_0^T = \rho_0$ | $\sigma_0 \rho_1^T = \rho_0$ | $\sigma_0 \rho_2 \rho_2^T = \rho_3$ | $\rho_4 \rho_3^T = \rho_3$ |
| $\rho_{r_k} \bar{\rho}_{r_k}^T =$ | $\rho_0 \rho_4^T = \rho_0$ | $\rho_1 \sigma_0^T = \rho_0$ | $\rho_2 \sigma_0^T = \rho_3$ | $\rho_3 \rho_4^T = \rho_3$ |
| $\rho_{r_k} \rho_{r_k}^T =$ | $\rho_0 \rho_0^T = \rho_0$ | $\rho_1 \rho_1^T = \rho_0$ | $\rho_2 \rho_2^T = \rho_3$ | $\rho_3 \rho_3^T = \rho_3$ |

TABLE III: A table to show that $\bar{\rho}_{r_k} \rho_{r_k}^T = \rho_{r_k} \bar{\rho}_{r_k}^T = \rho_{r_k} \rho_{r_k}^T$.

where we have used the mixed-product property. These relations can be simplified. First, since $\bar{\rho}_{r_k} \in \{\sigma_0, \sigma_3\}$, then $\bar{\rho}_{r_k} \bar{\rho}_{r_k}^T = I$ and therefore $\bar{\mathcal{A}} \bar{\mathcal{A}}^T = I$. Next, using the result from Table III, it follows that $\bar{\mathcal{A}} \mathcal{A}^T = \mathcal{A} \bar{\mathcal{A}}^T = \mathcal{A} \mathcal{A}^T$. Putting this all together yields $\mathcal{A}^c \mathcal{A}^{cT} = I - \mathcal{A} \mathcal{A}^T$. Using these same properties we have

$$\mathcal{A}^c \mathcal{A}^T = (\bar{\mathcal{A}} - \mathcal{A}) \mathcal{A}^T = \bar{\mathcal{A}} \mathcal{A}^T - \mathcal{A} \mathcal{A}^T = 0,$$

and

$$\mathcal{A} \mathcal{A}^{cT} = \mathcal{A} (\bar{\mathcal{A}}^T - \mathcal{A}^T) = \mathcal{A} \bar{\mathcal{A}}^T - \mathcal{A} \mathcal{A}^T = 0.$$

Finally, by evaluating the expressions for $\mathcal{A}^c \mathcal{A}^{cT}$, $\mathcal{A}^c \mathcal{A}^T$, and $\mathcal{A} \mathcal{A}^{cT}$ into (E1) we find that $U U^T = I$ as expected. Furthermore, $U U^T = I \implies U^T = U^{-1}$ since its inverse is unique, which proves that U is unitary by definition. \square

Appendix F: Proof for Theorem 2

Proof. First, we show that $U = U_1 U_2$. By expanding $U_1 U_2$ out we can see that $U = U_1 U_2$ if two conditions are met: $\mathcal{A} = \mathcal{A} \mathcal{A}^T \bar{\mathcal{A}}$ and $\mathcal{A}^c = (I - \mathcal{A} \mathcal{A}^T) \bar{\mathcal{A}}$. In Appendix E it was shown that $\mathcal{A} \mathcal{A}^T = \mathcal{A} \bar{\mathcal{A}}^T$ and $\bar{\mathcal{A}}^T \bar{\mathcal{A}} = I$. Using these relations together gives $\mathcal{A} \mathcal{A}^T \bar{\mathcal{A}} = \mathcal{A} \bar{\mathcal{A}}^T \bar{\mathcal{A}} = \mathcal{A} I = \mathcal{A}$. From this, it follows that $(I - \mathcal{A} \mathcal{A}^T) \bar{\mathcal{A}} = \bar{\mathcal{A}} - \mathcal{A} \mathcal{A}^T \bar{\mathcal{A}} = \bar{\mathcal{A}} - \mathcal{A} = \mathcal{A}^c$, where the last step is given in Definition 1. Since both conditions are met, it holds that $U = U_1 U_2$.

Next, we show that both U_1 and U_2 are unitary. Since all of the matrices used in our particular decomposition are real, the conjugate transpose is equivalent to the transpose. Starting with U_1 we have

$$U_1 U_1^T = \begin{pmatrix} (I - \mathcal{A} \mathcal{A}^T)^2 + \mathcal{A} \mathcal{A}^T \mathcal{A} \mathcal{A}^T & 2(\mathcal{A} \mathcal{A}^T - \mathcal{A} \mathcal{A}^T \mathcal{A} \mathcal{A}^T) \\ 2(\mathcal{A} \mathcal{A}^T - \mathcal{A} \mathcal{A}^T \mathcal{A} \mathcal{A}^T) & (I - \mathcal{A} \mathcal{A}^T)^2 + \mathcal{A} \mathcal{A}^T \mathcal{A} \mathcal{A}^T \end{pmatrix}.$$

By (23) we have

$$\mathcal{A} \mathcal{A}^T = \left(\bigotimes_{k=0}^{Q_1-1} \rho_{r_k} \rho_{r_k}^T \right) \otimes \mathcal{D} \otimes I_{n_x}^{\otimes j-1}. \quad (\text{F1})$$

Using the fact that $(\rho_{r_k} \rho_{r_k}^T) \in \{\rho_0, \rho_3, \rho_4\}$ for $r_k \in \{0, \dots, 4\}$, it follows that $\mathcal{A} \mathcal{A}^T$ is idempotent such that $\mathcal{A} \mathcal{A}^T \mathcal{A} \mathcal{A}^T = \mathcal{A} \mathcal{A}^T$. From this property it follows that $\mathcal{A} \mathcal{A}^T - \mathcal{A} \mathcal{A}^T \mathcal{A} \mathcal{A}^T = 0$ and $(I - \mathcal{A} \mathcal{A}^T)^2 + \mathcal{A} \mathcal{A}^T \mathcal{A} \mathcal{A}^T = I$ so $U_1 U_1^T = I$. Since $U_1 = U_1^T$ it follows that $U_1^T U_1 = U_1 U_1^T$ and therefore U_1 is unitary.

Finally, to show that U_2 is unitary we first note that $\bar{\mathcal{A}}$ as defined in (24) is unitary. Then we have

$$U_2 U_2^T = \begin{pmatrix} \bar{\mathcal{A}} & 0 \\ 0 & \bar{\mathcal{A}} \end{pmatrix} \begin{pmatrix} \bar{\mathcal{A}}^T & 0 \\ 0 & \bar{\mathcal{A}}^T \end{pmatrix} = \begin{pmatrix} \bar{\mathcal{A}} \bar{\mathcal{A}}^T & 0 \\ 0 & \bar{\mathcal{A}} \bar{\mathcal{A}}^T \end{pmatrix} = I,$$

where we once again use the property that $\bar{\mathcal{A}} \bar{\mathcal{A}}^T = I$. Since the inverse is unique, it follows that $U_2 U_2^T = U_2^T U_2$ and, therefore, U_2 is also unitary. \square

-
- [1] L. N. Trefethen, *Finite difference and spectral methods for ordinary and partial differential equations* (Cornell University-Department of Computer Science and Center for Applied . . . , 1996).
- [2] J. C. Strikwerda, *Finite Difference Schemes and Partial Differential Equations, Second Edition* (Society for Industrial and Applied Mathematics, 2004).
- [3] J. W. Thomas, *Numerical Partial Differential Equations: Finite Difference Methods* (Springer New York, 1995).
- [4] J. H. Ferziger and M. Perić, *Computational Methods for Fluid Dynamics* (Springer Berlin Heidelberg, 2002).
- [5] S. B. Pope, Turbulent flows, *Measurement Science and Technology* **12**, 2020–2021 (2001).
- [6] P. Bauer, A. Thorpe, and G. Brunet, The quiet revolution of numerical weather prediction, *Nature* **525**, 47–55 (2015).
- [7] T. N. Palmer, A nonlinear dynamical perspective on model error: A proposal for non-local stochastic-dynamic parametrization in weather and climate prediction models, *Quarterly Journal of the Royal Meteorological Society* **127**, 279–304 (2001).
- [8] J. Dudhia, A history of mesoscale model development, *Asia-Pacific Journal of Atmospheric Sciences* **50**, 121–131 (2014).
- [9] A. Montanaro, Quantum algorithms: an overview, *npj Quantum Information* **2**, 10.1038/npjqi.2015.23 (2016).
- [10] R. Babbush, D. W. Berry, R. Kothari, R. D. Somma, and N. Wiebe, Exponential quantum speedup in simulating coupled classical oscillators, *Physical Review X* **13**, 10.1103/physrevx.13.041041 (2023).
- [11] A. M. Dalzell, S. McArdle, M. Berta, P. Bienias, C.-F. Chen, A. Gilyén, C. T. Hann, M. J. Kastoryano, E. T. Khabiboulline, A. Kubica, *et al.*, Quantum algorithms: A survey of applications and end-to-end complexities, *arXiv preprint arXiv:2310.03011* (2023).
- [12] C. Bravo-Prieto, R. LaRose, M. Cerezo, Y. Subasi, L. Cincio, and P. J. Coles, Variational quantum linear solver, *Quantum* **7**, 1188 (2023).
- [13] A. W. Harrow, A. Hassidim, and S. Lloyd, Quantum algorithm for linear systems of equations, *Physical Review Letters* **103**, 10.1103/physrevlett.103.150502 (2009).
- [14] A. M. Childs, R. Kothari, and R. D. Somma, Quantum algorithm for systems of linear equations with exponentially improved dependence on precision, *SIAM Journal on Computing* **46**, 1920–1950 (2017).
- [15] H.-Y. Huang, K. Bharti, and P. Rebentrost, Near-term quantum algorithms for linear systems of equations with regression loss functions, *New Journal of Physics* **23**, 113021 (2021).
- [16] J.-P. Liu, H. Ø. Kolden, H. K. Krovi, N. F. Loureiro, K. Trivisa, and A. M. Childs, Efficient quantum algorithm for dissipative nonlinear differential equations, *Proceedings of the National Academy of Sciences* **118**, 10.1073/pnas.2026805118 (2021).
- [17] R. Demirdjian, D. Gunlycke, C. A. Reynolds, J. D. Doyle, and S. Tafur, Variational quantum solutions to the advection–diffusion equation for applications in fluid dynamics, *Quantum Information Processing* **21**, 10.1007/s11128-022-03667-7 (2022).
- [18] X. Li, X. Yin, N. Wiebe, J. Chun, G. K. Schenter, M. S. Cheung, and J. Mülmenstädt, Potential quantum advantage for simulation of fluid dynamics, *Physical Review Research* **7**, 10.1103/physrevresearch.7.013036 (2025).
- [19] F. Gaitan, Finding flows of a navier–stokes fluid through quantum computing, *npj Quantum Information* **6**, 10.1038/s41534-020-00291-0 (2020).
- [20] M. Lubasch, J. Joo, P. Moinier, M. Kiffner, and D. Jaksch, Variational quantum algorithms for nonlinear problems, *Physical Review A* **101**, 10.1103/physreva.101.010301 (2020).
- [21] F. Oz, R. K. S. S. Vuppala, K. Kara, and F. Gaitan, Solving burgers’ equation with quantum computing, *Quantum Information Processing* **21**, 10.1007/s11128-021-03391-8 (2021).
- [22] N. Gourianov, M. Lubasch, S. Dolgov, Q. Y. van den Berg, H. Babae, P. Givi, M. Kiffner, and D. Jaksch, A quantum-inspired approach to exploit turbulence structures, *Nature Computational Science* **2**, 30–37 (2022).
- [23] L. Lapworth, A hybrid quantum-classical cfd methodology with benchmark hhl solutions, *arXiv preprint arXiv:2206.00419* (2022).
- [24] B. Ljubomir, Quantum algorithm for the navier–stokes equations by using the streamfunction-vorticity formulation and the lattice boltzmann method, *International Journal of Quantum Information* **20**, 10.1142/s0219749921500398 (2022).
- [25] F. Tennie and T. N. Palmer, Quantum computers for weather and climate prediction: The good, the bad, and the noisy, *Bulletin of the American Meteorological Society* **104**, E488–E500 (2023).
- [26] H. Krovi, Improved quantum algorithms for linear and nonlinear differential equations, *Quantum* **7**, 913 (2023).
- [27] Z. Song, R. Deaton, B. Gard, and S. H. Bryngelson, Incompressible navier–stokes solve on noisy quantum hardware via a hybrid quantum–classical scheme, *Computers & Fluids* **288**, 106507 (2025).
- [28] D. Jennings, M. Lostaglio, R. B. Lowrie, S. Pallister, and A. T. Sornborger, The cost of solving linear differential equations on a quantum computer: fast-forwarding to explicit resource counts, *Quantum* **8**, 1553 (2024).
- [29] J. Penuel, A. Katarbarwa, P. D. Johnson, C. Farquhar, Y. Cao, and M. C. Garrett, Feasibility of accelerating incompressible computational fluid dynamics simulations with fault-tolerant quantum computers, *arXiv preprint arXiv:2406.06323* (2024).
- [30] A. J. Pool, A. D. Somoza, C. Mc Keever, M. Lubasch, and B. Horstmann, Nonlinear dynamics as a ground-state solution on quantum computers, *Physical Review Research* **6**, 10.1103/physrevresearch.6.033257 (2024).
- [31] S. Jin and N. Liu, Quantum algorithms for nonlinear partial differential equations, *Bulletin des Sciences Mathématiques* **194**, 103457 (2024).
- [32] J. Gonzalez-Conde, D. Lewis, S. S. Bharadwaj, and M. Sanz, Quantum carleman linearization efficiency in nonlinear fluid dynamics, *Phys. Rev. Res.* **7**, 023254 (2025).
- [33] D. Lewis, S. Eidenbenz, B. Nadiga, and Y. Subaşı, Limitations for quantum algorithms to solve turbulent and chaotic systems, *Quantum* **8**, 1509 (2024).
- [34] A. Surana and A. Gnanasekaran, Variational quantum framework for partial differential equation constrained optimization, *ACM Transactions on Quantum Comput-*

- ing **7**, 1 (2025).
- [35] A. Gnanasekaran, A. Surana, and T. Sahai, Efficient quantum algorithms for nonlinear stochastic dynamical systems, in *2023 IEEE International Conference on Quantum Computing and Engineering (QCE)*, Vol. 02 (2023) pp. 66–75.
- [36] A. Gnanasekaran, A. Surana, and H. Zhu, Variational quantum framework for nonlinear pde constrained optimization using carleman linearization, arXiv preprint arXiv:2410.13688 (2024).
- [37] A. Surana, A. Gnanasekaran, and T. Sahai, An efficient quantum algorithm for simulating polynomial dynamical systems, *Quantum Information Processing* **23**, 10.1007/s11128-024-04311-2 (2024).
- [38] N. Gourianov, P. Givi, D. Jaksch, and S. B. Pope, Tensor networks enable the calculation of turbulence probability distributions, *Science Advances* **11**, eads5990 (2025), <https://www.science.org/doi/pdf/10.1126/sciadv.ads5990>.
- [39] A. M. Childs and N. Wiebe, Hamiltonian simulation using linear combinations of unitary operations, *Quantum Information and Computation* **12**, 10.26421/qic12.11-12 (2012).
- [40] D. Gunlycke, M. C. Palenik, A. R. Emmert, and S. A. Fischer, Efficient algorithm for generating pauli coordinates for an arbitrary linear operator, arXiv preprint arXiv:2011.08942 (2020).
- [41] Y. Sato, R. Kondo, S. Koide, H. Takamatsu, and N. Imoto, Variational quantum algorithm based on the minimum potential energy for solving the poisson equation, *Physical Review A* **104**, 10.1103/physreva.104.052409 (2021).
- [42] M. Ali and M. Kabel, Performance study of variational quantum algorithms for solving the poisson equation on a quantum computer, *Physical Review Applied* **20**, 10.1103/physrevapplied.20.014054 (2023).
- [43] J. Gonzalez-Conde, T. W. Watts, P. Rodriguez-Grasa, and M. Sanz, Efficient quantum amplitude encoding of polynomial functions, *Quantum* **8**, 1297 (2024).
- [44] J. Bae, G. Yoo, S. Nakamura, S. Ohnishi, and D. S. Kim, Hardware efficient decomposition of the laplace operator and its application to the helmholtz and the poisson equation on quantum computer, *Quantum Information Processing* **23**, 10.1007/s11128-024-04458-y (2024).
- [45] C. A. Williams, A. A. Gentile, V. E. Elfving, D. Berger, and O. Kyriienko, Quantum iterative methods for solving differential equations with application to computational fluid dynamics, *Advanced Quantum Technologies*, e00618 (2025).
- [46] T. Hogancamp, R. Demirdjian, and D. Gunlycke, A linear combination of unitaries decomposition for the laplace operator, arXiv preprint arXiv:2601.06370 (2026).
- [47] D. Jennings, K. Korzekwa, M. Lostaglio, A. T. Sornborger, Y. Subasi, and G. Wang, Quantum algorithms for general nonlinear dynamics based on the carleman embedding, arXiv preprint arXiv:2509.07155 (2025).
- [48] A. Gnanasekaran and A. Surana, Efficient variational quantum linear solver for structured sparse matrices, in *2024 IEEE International Conference on Quantum Computing and Engineering (QCE)* (IEEE, 2024) p. 199–210.
- [49] H.-L. Liu, Y.-S. Wu, L.-C. Wan, S.-J. Pan, S.-J. Qin, F. Gao, and Q.-Y. Wen, Variational quantum algorithm for the poisson equation, *Physical Review A* **104**, 10.1103/physreva.104.022418 (2021).
- [50] A. Gnanasekaran and A. Surana, Efficient quantum access model for sparse structured matrices using linear combination of things, arXiv preprint arXiv:2507.03714 (2025).
- [51] M. A. Nielsen and I. L. Chuang, *Quantum Computation and Quantum Information: 10th Anniversary Edition* (Cambridge University Press, 2012).
- [52] E. Thula, Quantum incrementer (2024).
- [53] T. L. Scholten, C. J. Williams, D. Moody, M. Mosca, W. Hurley, W. J. Zeng, M. Troyer, J. M. Gambetta, T. Scholten, C. Williams, *et al.*, Assessing the benefits and risks of quantum computers (2024), arXiv preprint arXiv:2401.16317 (2024).
- [54] C. Gidney, Constructing large controlled nots (2015).
- [55] P. MQ Cruz and B. Murta, Shallow unitary decompositions of quantum fredkin and toffoli gates for connectivity-aware equivalent circuit averaging, *APL Quantum* **1** (2024).
- [56] Y. Hardy and W. Steeb, Decomposing the swap quantum gate, *Journal of Physics A: Mathematical and General* **39**, 1463 (2006).
- [57] A. Kay, Tutorial on the quantikz package, arXiv preprint arXiv:1809.03842 (2018).
- [58] M. Larocca, S. Thanasilp, S. Wang, K. Sharma, J. Biamente, P. J. Coles, L. Cincio, J. R. McClean, Z. Holmes, and M. Cerezo, Barren plateaus in variational quantum computing, *Nature Reviews Physics*, 1 (2025).
- [59] S. Sim, P. D. Johnson, and A. Aspuru-Guzik, Expressibility and entangling capability of parameterized quantum circuits for hybrid quantum-classical algorithms, *Advanced Quantum Technologies* **2**, 1900070 (2019).
- [60] H. Singh, S. Majumder, and S. Mishra, Benchmarking of different optimizers in the variational quantum algorithms for applications in quantum chemistry, *The Journal of Chemical Physics* **159** (2023).
- [61] Wikipedia, Commutation matrix — Wikipedia, the free encyclopedia, <http://en.wikipedia.org/w/index.php?title=Commutation%20matrix&oldid=1271312646> (2025), [Online; accessed 28-February-2025].
- [62] J. Watrous, *The Theory of Quantum Information* (Cambridge University Press, 2018).
- [63] C. Gidney, Simple algorithm for multiplicative inverses mod 2^n (2017).